

PROJECT ADMINISTRATION DATA SHEET

ORIGINAL



REVISION NO. \_\_\_\_\_

Project No. E-21-619DATE 3/25/82Project Director: R. W. SchaferSchool/Lab XXXX Electrical Eng.Sponsor: IBM Corp., Poughkeepsie, NYType Agreement: P.O. 956512 (Ltr. Agreement dated 2/1/82)Award Period: From 1/1/82 To 12/31/82 (Performance) 1/31/83 (Reports)Sponsor Amount: \$40,8444/36/83

Contracted through:

Cost Sharing: None

GTRI/ST

Title: Digital Signal Processing for In Situ Acoustical Noise MeasurementsADMINISTRATIVE DATAOCA Contact William F. Brown x4820

## 1) Sponsor Technical Contact:

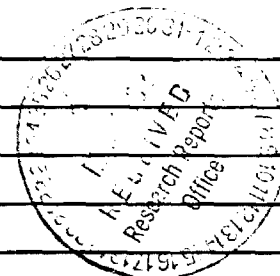
Mr. W. W. LangDept. C-18/Bldg. 704P. O. Box 390Poughkeepsie, NY 12602(914) 463-6380

## 2) Sponsor Admin/Contractual Matters:

Mr. Frank NagyDept. 672/Bldg. 415IBM CorporationP. O. Box 950, Poughkeepsie, NY 12602(914) 463-1912Defense Priority Rating: noneSecurity Classification: noneRESTRICTIONS

See Attached \_\_\_\_\_ Supplemental Information Sheet for Additional Requirements.

Travel: Foreign travel must have prior approval -- Contact OCA in each case. Domestic travel requires sponsor approval where total will exceed greater of \$500 or 125% of approved proposal budget category.

Equipment: Title vests with none proposed or anticipatedCOMMENTS:COPIES TO:

RAN  
Administrative-Coordinators  
Research Property Management  
Accounting  
Procurement/EES Supply Services

Research Security Services  
Reports Coordinator (OCA)  
Legal Services (OCA)  
Library

EES Public Relations (2)  
Computer Input  
Project File  
Other \_\_\_\_\_

SPONSORED PROJECT TERMINATION SHEETDate 4/13/83

Project Title: Digital Signal Processing for In Situ Acoustical Noise Measurements

Project No: E-21-619

Project Director: R. W. Schafer

Sponsor: IBM Corp., Poughkeepsie, NY

Effective Termination Date: 4/30/83Clearance of Accounting Charges: 4/30/83

Grant/Contract Closeout Actions Remaining:

- ☒ Final Invoice and ~~Other Documents~~
- ☐ Final Fiscal Report
- ☐ Final Report of Inventions
- ☐ Govt. Property Inventory & Related Certificate
- ☐ Classified Material Certificate
- ☐ Other \_\_\_\_\_

Assigned to: Electrical Engineering (School/~~Laboratory~~)COPIES TO:

Research Administrative Network  
~~Administrative Coordinator~~  
Research Property Management  
Accounting  
Procurement/EES Supply Services

Research Security Services  
~~Reports Coordinator (OCA)~~  
Legal Services (OCA)  
Library

EES Public Relations (2)  
Computer Input  
Project File  
Other \_\_\_\_\_



GEORGIA INSTITUTE OF TECHNOLOGY  
SCHOOL OF ELECTRICAL ENGINEERING  
ATLANTA, GEORGIA 30332

ONE: (404) 894-2961

April 27, 1982

Mr. Frank Nagy  
Dept. 672/Bldg. 415  
IBM Corporation  
P.O. Box 950  
Poughkeepsie, NY 12602

SUBJECT: Quarterly Status Report, "Digital Signal Processing for  
Situ Acoustical Noise Measurements", (Letter Agreement  
dated 2/1/82 between Georgia Institute of Technology and  
IBM Corp.)  
Period Covered - 1/1/82 - 3/31/82

Dear Mr. Nagy:

The subject report is forwarded in conformance with contract specifications.

Should you have any questions or comments regarding this report, please feel free to contact me at (404) 894-2961.

Sincerely,

Administrative Asst.

Enclosure  
MS/rr



College of Engineering  
School of Electrical Engineering  
Digital Signal Processing Laboratory

Quarterly Status Report  
on  
Digital Signal Processing for In Situ  
Acoustical Noise Measurements

by

Ronald W. Schafer

Period Covered by Report

January 1, 1982 through March 31, 1982

Personnel Working on Project

Ronald W. Schafer, Regents' Professor  
Elisabet Andresdottir, Graduate Assistant

Research Activities During Report Period

The project was initiated during this quarter. Activities were focused upon the development of basic signal processing programs that will be used during the course of the research project. Some work was also devoted to locating and becoming familiar with the standards for acoustic noise measurement.

Accomplishments During Report Period

Computer programs were written and tested for the following signal processing and simulation functions:

- (1) Simulation of impulse response of a reverberant room. A program now exists for the computation of impulse response of a reverberant room according to the algorithm published by Allen and Berkley (JASA, 65, 1979, pp. 943-950). The program allows simulations of various room sizes, sound absorption properties and various locations of source and microphone.
- (2) Digital Filter Implementation Program. A program for convolution of a room impulse response with an input noise signal has been written and tested. The program uses FFT convolution techniques to implement filtering with impulse responses up to 2048 samples long.

- (3) Dereverberation Program. A program based upon the two-microphone system of Allen, Berkley and Blanert, [JASA, 62, No. 4, October 1977, pp. 912-915] has been written and is currently being tested. This program has built-in options for measuring power spectra of the input microphone signals and the resulting dereverberated output spectrum as well as the capability for resynthesizing a dereverberated time waveform.

Projected Work for Next Quarter

Work will now turn toward simulations of acoustic noise measurements in a reverberant environment. The programs described above will permit us to simulate a wide variety of measurement situations and to experiment with the multi-microphone method of reverberation correction. We shall also be working with the staff of the IBM Acoustics Lab regarding measurements of typical noise emitting machines.

4-761-211

DIGITAL SIGNAL PROCESSING FOR "IN SITU"  
ACOUSTICAL NOISE MEASUREMENTS

A THESIS  
Presented to  
The Faculty of the Division of Graduate Studies  
by  
Elisabet Andresdottir

In Partial Fulfillment  
of the Requirements for the Degree  
Master of Science in Electrical Engineering

Georgia Institute of Technology

March 1983

DIGITAL SIGNAL PROCESSING FOR "IN SITU"  
ACOUSTICAL NOISE MEASUREMENTS

A THESIS

Presented to

The Faculty of the Division of Graduate Studies

by

Elisabet Andresdottir

In Partial Fulfillment

of the Requirements for the Degree

Master of Science in Electrical Engineering

Georgia Institute of Technology

March 1983

## Summary

### Digital Signal Processing for "In Situ" Acoustical Noise Measurements

Elisabet Andresdottir

80 Pages

Directed by Dr. R.W. Schafer

In order to make precise measurements of machine noise emissions, a controlled acoustical environment such as hemi-anechoic room or nonreverberant room is required by current technology.

This thesis is a study of techniques for processing signals, measured in "in situ" environment, that is, in a noisy reverberant room, so as to remove the effect of background noise and room reflections from the measurement. In this aspect, three techniques are studied; nonadaptive beamformer, constrained adaptive beamformer and adaptive noise canceller. Measurements are simulated on a computer and the performance of the different techniques is discussed. A new approach for deriving the constrained optimum solution is formulated by using properties of projections and subspaces in Hilbert spaces.

The results of this research indicate that significant improvement can be accomplished by using nonadaptive equally weighted beamformers to reduce the effect of reverberation.



The adaptive processors improve the results significantly over those of the nonadaptive processor, when there is a strong undesired signal source in the room.

DIGITAL SIGNAL PROCESSING FOR "IN SITU"  
ACOUSTICAL NOISE MEASUREMENTS

Approved :

\_\_\_\_\_  
Ronald W. Schafer, Chairman

\_\_\_\_\_  
Russell M. Mersereau

\_\_\_\_\_  
Monson H. Hayes

Date approved by Chairman : \_\_\_\_\_

Dedicated to

my parents

Andres and Audur

and my brothers and sister

Eirikur, Gunnar and Vala

## ACKNOWLEDGEMENT

I am very grateful for having had the opportunity to work with the whole DSP group, both professors and students. It has been an enjoyable time and I am grateful to everyone in the group for always being ready to help or advice when needed. Specially I want to thank Dr. Ronald W. Schafer for his advice and guidance during the course of the research. I also want to thank him and the other professors in the group for having created the good atmosphere on the fourth floor, that we, the students, enjoyed so richly. I want to thank Dr. Russell M. Mersereau for very helpful hints when serving on my reading committee. I want to thank Dr. Thomas P Barnwell for always being ready to help, no matter what time of day or week. (I also want to thank him for his part in making the DSP seminars fun to attend). I want to thank Chris Hodges and Charles Gimark for their help when the computer had its bad days. Finally, I want to thank all my office mates for a great time, especially my husband Lindi, who has encouraged and supported me.

My Master's studies were enabled by a Research Assistantship under Dr. R. W. Schafer, supported by the IBM corporation, for which I am very grateful.

## LIST OF TABLES

Table		Page
1 - Standard Center, Lower and Upper Frequencies for Octave and 1/3 Octave Bands . . . . .		32
2 - A Comparison between Nonadaptive Equally Weighted Beamformer and Constrained Adaptive Beamformer in a Reverberant Room . . . . .		60
3 - Performance of the Nonadaptive Equally Weighted Beamformer in a Reverberant Environment . . . . .		61
4 - A Comparison between Nonadaptive Equally Weighted Beamformer and Constrained Adaptive Beamformer in a Noisy Reverberant Environment . . . . .		62
5 - A Test of Performance by Varying Processor Parameters . . . . .		63
6 - A Comparison between the three Processing Techniques Using 4 and 5 Microphones Array in a Noisy Reverberant Environment . . . . .		64
7 - A Test of Performance by Varying Processor Parameters and a Comparison between the three Different Processing Techniques in a Noisy Reverberant Environment . . . . .		67

## LIST OF ILLUSTRATIONS

Figure		Page
1.	Illustration of Machine Noise Measurements . . . . .	2
2.	Nonadaptive Beamformer . . . . .	8
3.	Arrival of an Undesired Source Signal at the Microphone Array. . . . .	13
4.	Curved Wavefront Arriving at the Microphone Array . . . . .	16
5.	An Array Pattern for equally Weighted Uniformly Spaced Microphone Array for a Planar Wavefront. . . . .	19
6.	Constrained Adaptive Beamformer . . . . .	19
7.	Equivalent Processor for the Desired Direction . . . . .	19
8.	Adaptive Noise Cancelling . . . . .	25
9.	Model of the Transfer Function the Desired and Undesired Signals through the Adaptive Noise Cancelling. . . . .	26
10.	Frequency Dependent Thresholds of Hearing and Feeling for People with Acute Hearing . . . . .	34
11.	Relative Response Functions for A, B, and C Weightings . . . . .	36
12.	Reverberant Decay of Running Time Average of Square of Acoustic Pressure as Displayed by a High-Speed Level Recorder . . . . .	39
13.	Sound-Pressure Level (Relative to that of Reverberant Field) versus Ratio of Distance, $r$ ,	

	from Source to Radius of Reverberation, $r$ . . . . .	42
14.	Model of the Procedure for the Simulated Measurements . . . . .	44
15.	Example of a Simulated Room Impulse Response . . . . .	46
16.	Convergence of the output Power for one of the Cases . . . . .	50

## TABLE OF CONTENTS

	Page
ACKNOWLEDGEMENTS . . . . .	ii
LIST OF TABLES . . . . .	iii
LIST OF ILLUSTRATIONS . . . . .	iv
CHAPTER	
I. INTRODUCTION . . . . .	1
II. BACKGROUND . . . . .	6
III. BEAMFORMING . . . . .	11
Nonadaptive Beamforming	
Adaptive Beamforming	
Adaptive Noise Cancelling	
IV. ACOUSTIC NOISE MEASUREMENTS . . . . .	30
V. ROOM ACOUSTICS . . . . .	38
VI. SIMULATIONS . . . . .	43
VII. EXPERIMENTS . . . . .	48
Measurement Parameters	
Processor Parameters	
Experimental Results	
Introduction	
Desired Source + Reverberation	
Desired Source + Reverberation +	
Undesired Source	



## Computer Time Considerations

VIII.	CONCLUSIONS AND RECOMMENDATIONS . . .	69
	Conclusions	
	Recommendations	
APPENDIX	. . . . .	72
BIBLIOGRAPHY	. . . . .	79

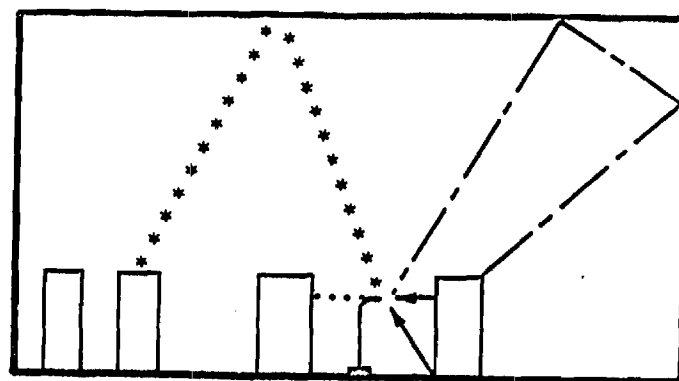
## CHAPTER I

### INTRODUCTION

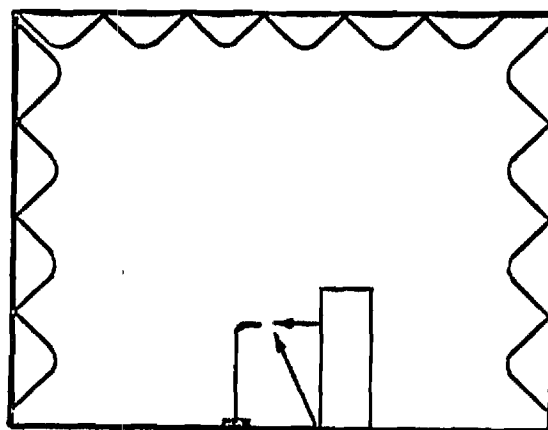
There is a need for the development of quieter data processing equipment, which, in turn, requires reliable methods for measurement of the noise emitted by individual machines.

In order to make precise measurements of machine noise emissions, a controlled acoustical environment such as hemi-anechoic room or nonreverberant room is required by current technology. The purpose of this study is to explore the use of digital signal processing techniques for making precise noise emission measurements in an "in situ" environment. The emphasis will be on using digital signal processing methods to remove the effects of unwanted reflections from the walls and to remove the effects of background noise. Essentially, the object is to convert an "in situ" environment into an anechoic or hemi-anechoic environment.

The problem is depicted in more detail in Figure 1. In Figure 1a, the solid paths (—) indicate sound energy received directly from one (or more ) sources in the machine. The path denoted by (----) illustrates reflected



(a)



(b)

Figure 1 Illustration of Machine Noise Measurements in  
(a) a Real Room and (b) a Hemi-Anechoic Room

sound energy from the machine under test, and ( . . . . ) illustrates sound energy from another machine which is background noise. ( \* \* \* ) represents additional background noise reflected from the ceiling of the real room. In Figure 1b, the measurements are made in a hemi- anechoic room in the absence of other machines so that reflected energy and background noise are not present.

We have studied techniques for processing the signals received from an array of microphones so as to reduce the effects of background noise and room reflections in the measurement. It is anticipated that the development of such a system would save considerable time in the evaluation of machine noise, and would make possible the testing of equipment that operates in an interactive mode with other equipment in situations where it is not possible to move all of the equipment to a controlled acoustical environment. In this study no real noise measurements were made, due to the complexity of the measurement apparatus required for multi-channel recording of acoustic signals. Instead all the measurements are simulated on a computer. An "in situ" environment is simulated by using an existing algorithm [1] for computing the impulse response of a simulated reverberant room. After processing the simulated measured signal, its A-weighted power level for each octave band is calculated and compared to the A-weighted power levels of

the desired signal. The results show that significant improvement can be accomplished by using beamformers. The beam is steered towards the desired signal source and by using different kinds of cancelling methods the undesired signal is reduced. Three kinds of beamforming techniques were studied and applied to the described problem. One of these techniques, constrained adaptive beamforming, requires solving an optimization problem with constraints. In solving that problem a new approach was taken by using the properties of projections and subspaces in Hilbert spaces.

This thesis report is divided into 8 chapters. Chapter II gives a brief summary of how such problems have been approached in the past, and states some new approaches to this problem based upon approaches that have been used in similar sonar and radar problems. Chapter III gives a detailed analysis of three techniques that were investigated in detail. The three techniques are: nonadaptive equally weighted beamforming, constrained adaptive beamforming [2], and adaptive noise cancelling [3]. Chapter IV briefly summarizes principles of standard acoustic noise measurements which were followed in our simulations. Chapter V deals with room acoustics, where some concepts of reverberation are explained. Chapter VI gives a detailed description of how the simulations of the measurements are conducted, as well as how the processing procedures are

implemented. In chapter VII the choice of different parameters for the processing techniques is discussed as well as the design of the room and the choice of the measurement parameters. The results of the different processing techniques are summarized and discussed for a wide range of parameters. Finally in chapter VIII we discuss some conclusions that can be made from the results, what can be accomplished using the different techniques, and the weak points of each technique. In addition it includes some suggestions for future work.

## CHAPTER II

### BACKGROUND

Current techniques for the measurement of noise emissions of computer and business equipment require measurement of the sound pressure level in a hemi-anechoic acoustical environment [4]. The sound pressure level at a bystander position may be of interest or the sound power measured according to current international standards [5-8] may be determined. These procedures require measurements of the sound pressure at points near the machine that are free from the effects of background noise and from reflected signals such as those reflected from room surfaces or other machines in the vicinity. These measurements generally require a hemi-anechoic room so that the only reflecting plane is the floor; background noise can be neglected. In some cases, [9] one can correct for background noise and for the presence of room reflections, but the allowed corrections are small. The effects of reflections are assessed in a real room by determining the sound power of a reference source (which produces a known sound power) and using the difference between the measured and known values to correct measurements of a source of unknown sound power. But these corrections are small and do not allow accurate

data to be obtained in "in situ" environments. Precision measurements require different approach.

The goal of this thesis work is to investigate techniques for reduction of the effects of unwanted reflections and background noise from the sound pressure levels measured at an array of positions produced by a source (such as a computer) in a real room. The transmission path between the source and receiver in a room is complex and is highly dependent on the source position in the room. The removal of background noise is complicated by the fact that the statistics of the background noise are not appreciably different from the statistics of the noise produced by the machine.

Similar problems arise in radar and sonar signal processing. In these areas, arrays of sensors have been used to attempt to discriminate against undesired jammer signals. The book "Introduction to Adaptive Arrays" [10] is a good summary of what has been done in that field. In particular Frost [2] has published a very sophisticated but powerful algorithm for a broadband adaptive beamformer. In cases of low signal to noise ratio the noise cancelling algorithm developed by Widrow [3] may be applicable.

In this thesis work an attempt is made to apply the existing theory of radar and sonar signal processing to the above mentioned problem of acoustic noise measurement in a noisy reverberant environment.



## CHAPTER III

## BEAMFORMING

Nonadaptive Beamforming

Beamforming can be a useful concept when one wants to distinguish a signal coming from one direction from signals coming from other directions. By using an array of microphones with the signal received at each microphone given a specific delay and weighting, beamforming can be accomplished. Figure 2 shows the basic beamforming process.

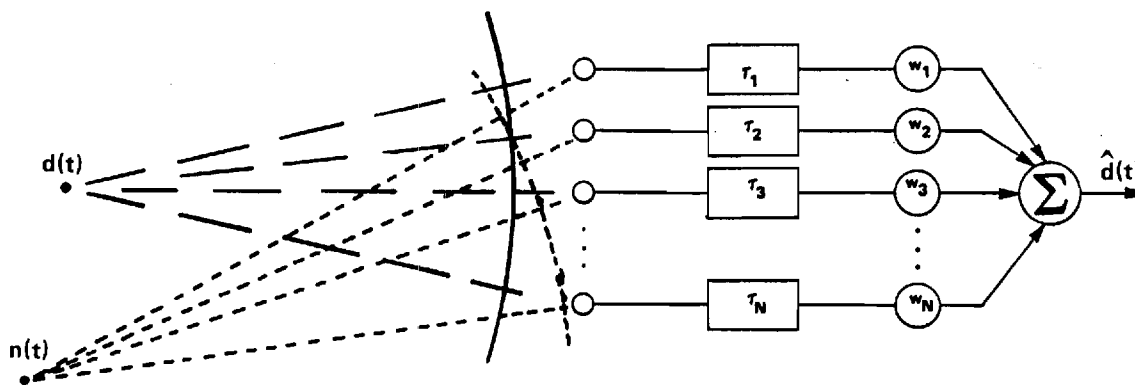


Figure 2 Nonadaptive Beamformer

If  $d(t)$  is the signal coming from the desired direction, the delays  $\tau_i$  are chosen such that  $d(t)$  will be added in phase. With that choice,  $n(t)$ , the undesired signal, will be added out of phase and will tend to cancel out. If the

weights,  $w_i$  are chosen such that

$$\sum_i w_i = 1 \quad (1)$$

then the signal from the desired direction passes through the beamformer with unity gain. With these constraints on  $w_i$ , one has  $N-1$  degrees of freedom in choosing the remaining  $w_i$ 's. These weights can be chosen so as to minimize the effects of signals from undesired directions. Using this approach, the estimate of the desired signal,  $\hat{d}(t)$ , is

$$\begin{aligned} d(t) &= \sum_{i=1}^N w_i (d_i(t-\tau_i) + n_i(t-\tau_i)) \\ &= \sum_{i=1}^N w_i d_i(t-\tau_i) + \sum_{i=1}^N w_i n_i(t-\tau_i) \end{aligned} \quad (2)$$

but

$$d_i(t-\tau_i) = d(t) \quad \text{all } i \quad (3)$$

and

$$\sum_i w_i = 1$$

hence

$$\hat{d}(t) = d(t) + \sum_{i=1}^N w_i n_i(t-\tau_i)$$

$$= d(t) + e(t) \quad (4)$$

where  $e(t)$  is the error term which is to be minimized. Since the  $\tau_i$ 's are fixed, and chosen to compensate for the different arrival times of the desired signal at different microphones, the amount of undesired-signal cancellation depends upon how far off  $n(t)$  is from the desired direction, the phase difference between  $n_i(t)$  and  $n_{i+1}(t)$ , i.e. the spacing of the microphones, and also upon the choice of the weights  $w_i$ .

One can write  $n_i(t) = n(t - \alpha_i)$  where  $\alpha_i$  depends on the direction from which the signal  $n(t)$  is coming. It follows that

$$\hat{d}_\theta(t) = d(t) + \sum_{i=1}^N w_i n(t - \alpha_i - \tau_i) \quad (5)$$

If we assume that  $n(t)$  has a planar wavefront at the microphone array, that is, the angle upon arrival,  $\theta$ , of the wavefront is the same at all the microphones, then we have

$$\alpha_i = \frac{(i-1) d \sin \theta}{c} \quad (6)$$

where  $c$  is the speed of sound in air, and  $d$  is the spacing between the microphones (see Figure 3).

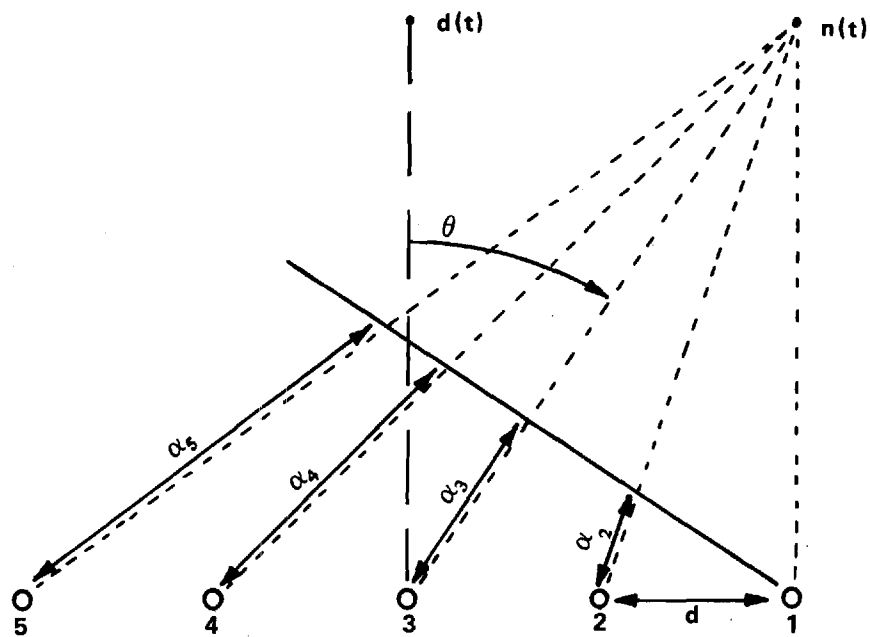


Figure 3 Arraival of an Undesired Source at the Microphone Array

The Fourier Transform of  $\hat{d}_\theta(t)$  is

$$D_\theta(\omega) = D(\omega) + \sum_{i=1}^N w_i N(\omega) e^{-j\omega(\alpha_i + \tau_i)} \quad (7)$$

$$= D(\omega) + \sum w_i N(\omega) e^{-j\omega \tau_i} e^{-j2\pi(i-1) \left(\frac{d}{\lambda}\right) \sin \theta}$$

$\theta$  is the angle between the desired signal direction and the undesired signal direction. If the desired direction is perpendicular to the microphone array then all the  $\tau_i$ 's are zero if the array is in the far field of the source. The far field assumption allows the incoming beam to be modelled as a plane wave. If the microphone array is in the near field of the source, then the  $\tau_i$ 's are used to compensate for the curvature of the wavefront as well as for the direction of the source. In this case the values of the  $\tau_i$ 's do not increase linearly with increasing  $i$  as they would in case of pure direction compensation.

Looking at equation (7) we see that our estimation  $D_\theta(\omega)$  depends upon both the frequency,  $\omega$ , and the angle  $\theta$  from the desired direction. Thus the array pattern is frequency dependent. If we hold the frequency fixed, say  $\omega = \omega_0$  then we get

$$\hat{D}_\theta(\omega_0) = D(\omega_0) + N(\omega_0) \underbrace{\sum_{i=1}^N w_i e^{-j\omega_0 \tau_i} e^{-j2\pi(i-1)(d/\lambda_0)\sin\theta}}_{AF_{\omega_0}(\theta)} \quad (8)$$

If  $D$  is the shortest distance from the desired source to the microphone array and the desired direction is perpendicular to the array, then for an odd number of microphones:

$$\tau_{\frac{N+1}{2}} \pm j = \frac{\sqrt{D^2 + (jd)^2} - D}{c} \quad j = 1, \dots, \frac{N-1}{2} \quad (9)$$

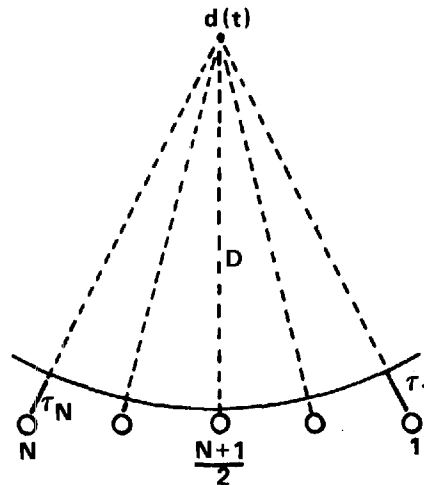


Figure 4 Curved Wavefront Arriving at the Microphone Array

By changing the index on the summation,

$$\begin{aligned}
 AF_{\omega_0}(\theta) &= \sum_{i=-\frac{N-1}{2}}^{\frac{N-1}{2}} w_i \exp(-j2\pi f_0 (\frac{\sqrt{D^2 + (id)^2}}{c} - D)) \exp(-j2\pi (i + \frac{N-1}{2})(d/\lambda_0) \sin \theta) \\
 &= \sum_{i=-\frac{N-1}{2}}^{\frac{N-1}{2}} w'_i \exp(-j2\pi (i + \frac{N-1}{2})(d/\lambda_0) \sin \theta)
 \end{aligned} \tag{10}$$

where

$$w'_i = w_i \exp(-j2\pi (\sqrt{(D/\lambda_0)^2 + (id/\lambda_0)^2} - D/\lambda_0)) \tag{11}$$

If the desired wavefront is planar then  $D^2 + (jd)^2 = D^2$  and all of the  $\tau_i$ 's are zero. In this case the equation for  $AF_{\omega_0}(\theta)$  reduces to

$$AF_{\omega_0}(\theta) = \sum_{i=-\frac{N-1}{2}}^{\frac{N-1}{2}} w_i \exp(-j2\pi (i - \frac{N-1}{2})(d/\lambda_0) \sin \theta) \tag{12}$$

If all the microphones have equal weights, the array factor simply becomes a geometric series:

$$AF_{\omega_0}(\theta) = 1/N \sum_{i=-\frac{N-1}{2}}^{\frac{N-1}{2}} \exp(-j2\pi (i - \frac{N-1}{2})(d/\lambda_0) \sin \theta) \tag{13}$$

$$= 1/N \exp(+j2\pi \frac{N-1}{2} (d/\lambda_0) \sin \theta) \frac{\sin[N/2 \cdot 2\pi (d/\lambda_0) \sin \theta]}{\sin[(2\pi/2)(d/\lambda_0) \sin \theta]}$$

Figure 5 shows plots of the array factor for different numbers of microphones.



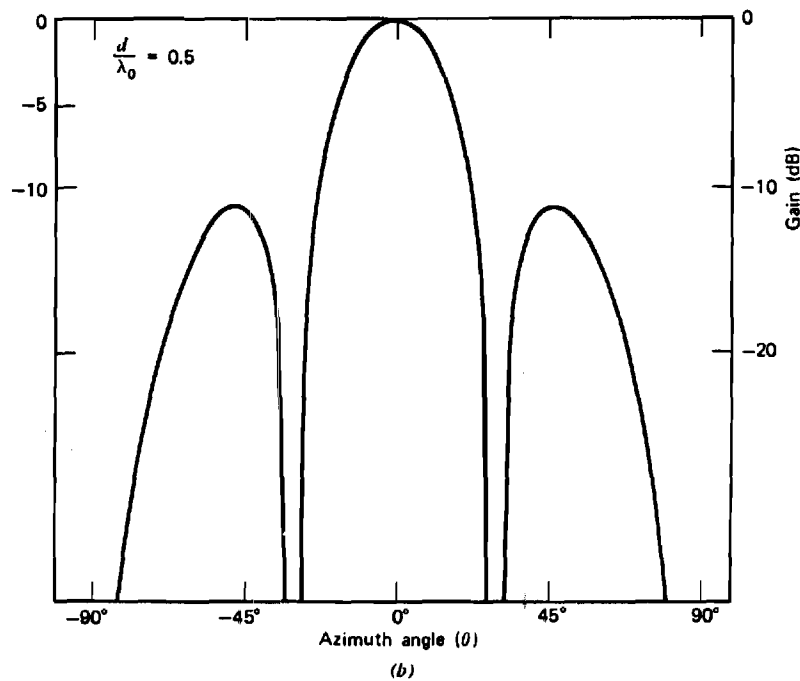
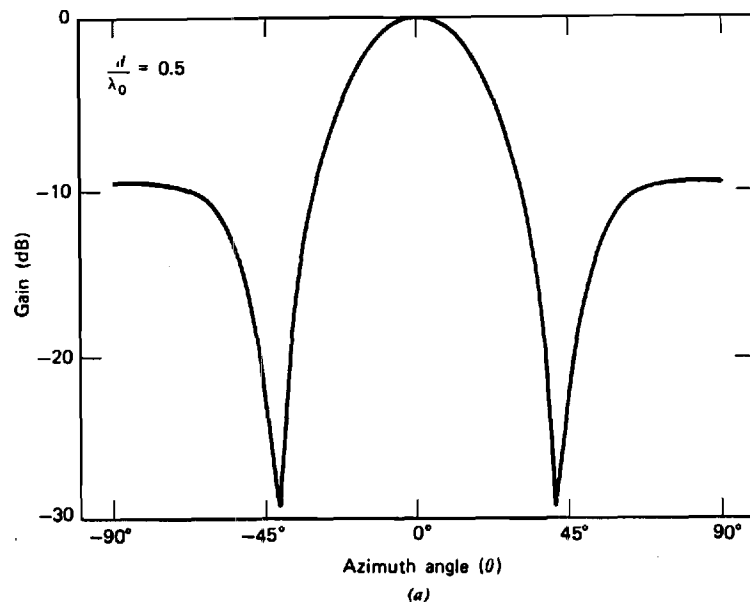
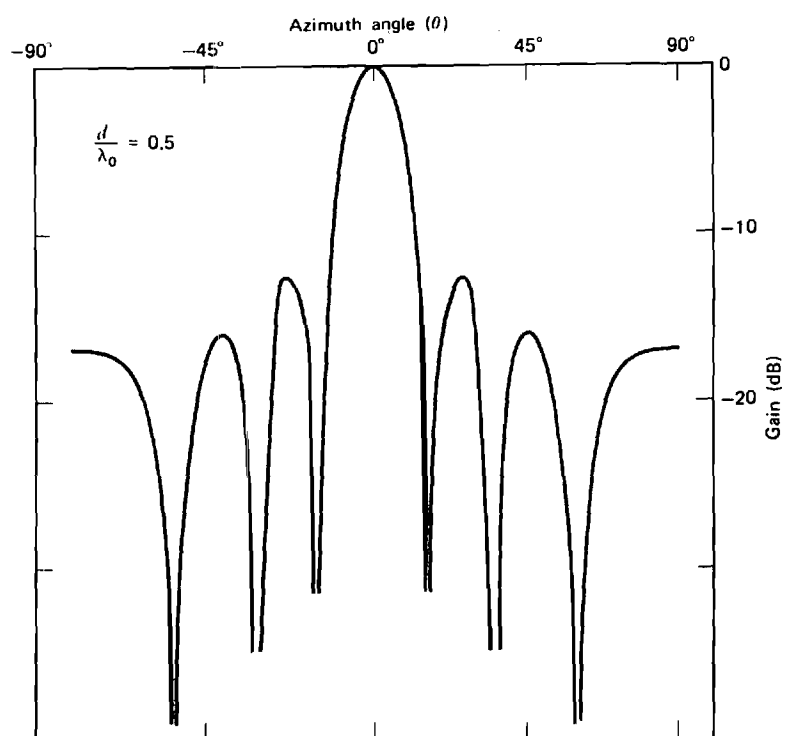
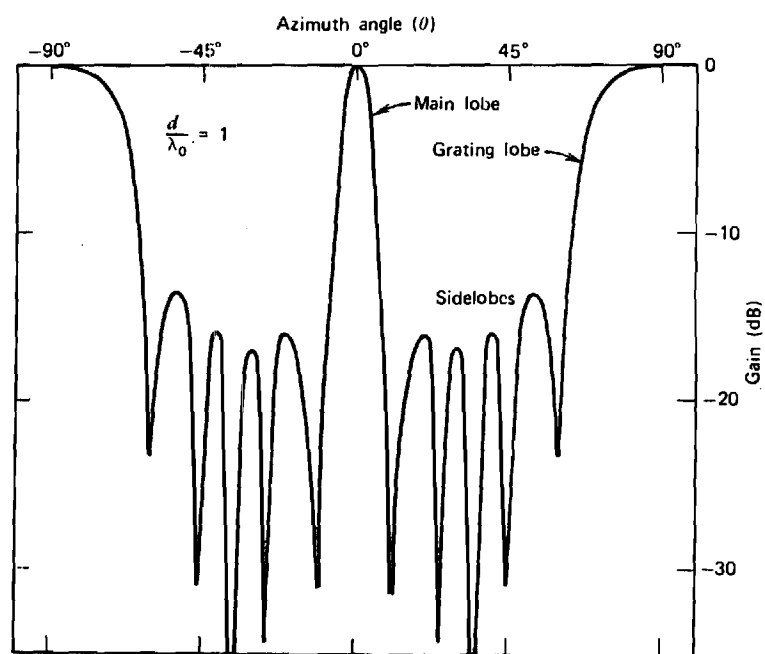


Figure 5 An array Pattern for Equally Weighted Uniformly Spaced Microphone array for a Planar Wavefront. (a) 3 Microphone Array (b) 4 Microphone Array (c) 7 Microphone Array (d) 7 Microphone Array with  $d/\lambda_0 = 1$



(c)



(d)

Figure 5 (continued)

### Adaptive Beamforming

Adaptive beamforming can be very useful when one does not know the direction to the undesired signals, and does not know therefore how to choose the weights in order to place nulls in the directions of undesired signals. Using an adaptive beamformer solves this problem.

When dealing with broad band signals, the spacing between the microphones in the array becomes a problem. For some fixed spacing the spatial resolution may be poor for certain frequencies, and at higher frequencies one may end up with grating lobes in the undesired direction as is shown in Figure 5-c. Frost [2] has published a very powerful but sophisticated algorithm for broad band signals. This algorithm imposes constraints on signals coming from the desired direction, i.e. the mean value of the output power is minimized, but with the constraint that the desired signal is filtered by a prescribed FIR filter. A block diagram of this algorithm is shown in Figure 6. Before the actual adaptive process starts, the beam is steered in the desired direction by giving the desired signal special delays at the different microphone inputs to compensate for any time differences of the desired signal wavefront appearing at the microphone array. The signal from the desired direction will therefore be in phase at each column

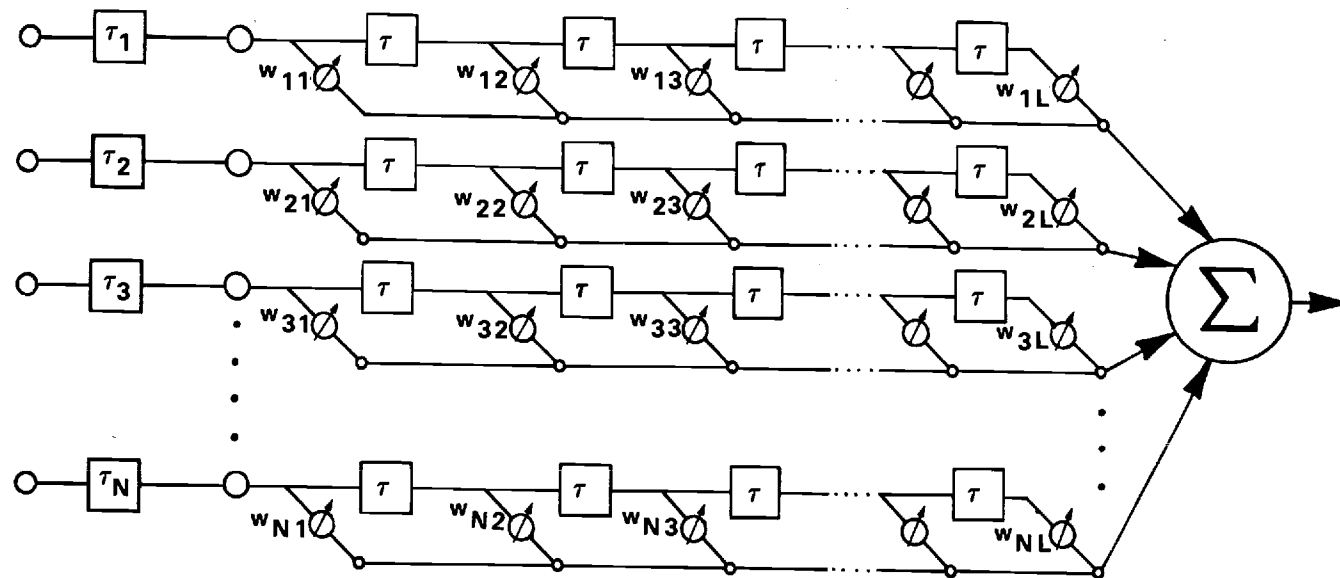


Figure 6 Constrained Adaptive Beamformer

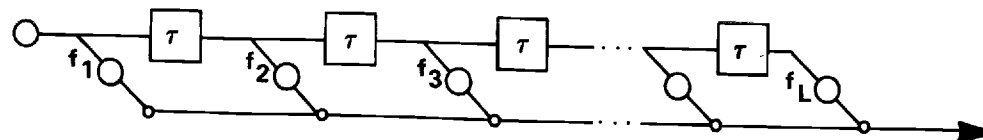


Figure 7 Equivalent Processor for the Desired Direction

$$w^T = [w_{11} \ w_{21} \ \dots \ w_{N1} \ w_{12} \ \dots \ w_{NL}] \quad (17)$$

and  $w_{ji}$  and  $x_{ji}(k)$  correspond to the weight and the input signal at time  $k$  at sensor  $j$  and at the  $(i-1)$  th delay down the tapped delay line. Define

$$R_{xx} = E[x(k) \ x(k)^T] \quad (18)$$

Now we want to minimize the effect of undesired signals in  $y(k)$  but without affecting the desired signal. By minimizing the output power with respect to  $w$  and with the constraint that the desired signal will not be affected, this can be accomplished. We have

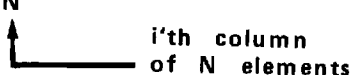
$$E[y(k)^2] = w^T R_{xx} w \quad (19)$$

Since the  $f_i$ 's are the sum of the weights in the  $i$ 'th column, one can force the weight vector  $w$  to satisfy the constraints on  $f_i$  by the requirement,

$$c_i^T w = f_i \quad i = 1, \dots, L \quad (20)$$

where

$$c_i^T = [\underbrace{0 \dots 0}_{N} \dots \underbrace{0 \dots 1 \dots 1}_{N} \dots 0 \dots 0]$$



down the tapped delay line. The direction of the desired signal must therefore be known, but that is all one has to know. A tapped delay line with adjustable weights is connected to each sensor. The weights are adaptively adjusted to minimize the mean value of the output power. Since the desired signal is in phase at each column down the rows of the tapped delay lines, the equivalent processor for the desired direction is an FIR filter as shown in Figure 7, where

$$f_i = \sum_{j=1}^N w_{ji} \quad i = 1, \dots, L \quad (14)$$

As in the case of nonadaptive beamformer in Figure 2, one can put constraints on the  $f_i$ 's of Figure 7. As a result the processor can minimize the output power while the signal coming from the desired direction is filtered by a controlled FIR transfer function.

If  $y(k)$  is the output of the adaptive beamformer at time  $k$ , then we can write

$$y(k) = x^T(k) w \quad (15)$$

where  $x(k)$  and  $w$  are the vectors,

$$x(k)^T = [x_{11}(k) \ x_{21}(k) \ \dots \ x_{N1}(k) \ \dots \ x_{NL}(k)] \quad (16)$$

By doing this for all the  $i$ 's we define the  $L \times NL$  matrix  $C$ , where

$$C = [c_1 \dots c_i \dots c_L] \quad (21)$$

and by writing

$$f = \begin{bmatrix} f_1 \\ f_2 \\ \vdots \\ f_L \end{bmatrix} \quad (22)$$

we have the constraints

$$C^T w = f \quad (23)$$

where  $f_i$  is the desired sum of all the  $w_{ji}$  down the  $i$ 'th column.

The minimization problem is therefore:

$$\begin{aligned}
 &\text{Minimize } w^T R_{xx} w \\
 &\text{subject to } C^T w = f
 \end{aligned}
 \tag{24}$$

The classical solution of this problem uses Lagrange multipliers to find the minimum that satisfies the constraints. In Appendix this problem is solved using a different approach; that is, by using projections and constrained subspaces. The solution of this problem is,

$$w_{\text{opt}} = R_{xx}^{-1} C (C^T R_{xx}^{-1} C)^{-1} f \tag{25}$$

Using the gradient algorithm, we can update the weighting coefficients using

$$w(k+1) = P_M [ w(k) - \mu x(k) y(k) ] + g \tag{26}$$

where  $P$  is defined as,

$$\begin{aligned}
 P_M &= I - C (C^T C)^{-1} C^T \\
 g &= C (C^T C)^{-1} f
 \end{aligned}$$

and as an initial condition,

$$w(0) = g$$

The conditions for the convergenco of the weight vector to



its optimum are derived by Frost [2]. The results of this derivation are that if the step size in the updating process is chosen such that

$$0 < \mu < \frac{2}{3 \operatorname{tr}(R_{xx})} \quad (27)$$

then the algorithm will converge. The trace of the matrix  $R_{xx}$ ,  $\operatorname{tr}(R_{xx})$ , is easy to calculate since it is the sum of all the tap power values.

### Adaptive Noise Cancelling

The adaptive algorithm described in section 3.2 is rather sophisticated and requires considerable processing time, but it is also very powerful. In cases where the undesired signals are stronger than the desired ones, an adaptive noise canceller [3], which is much simpler than the adaptive beamformer may be applicable.

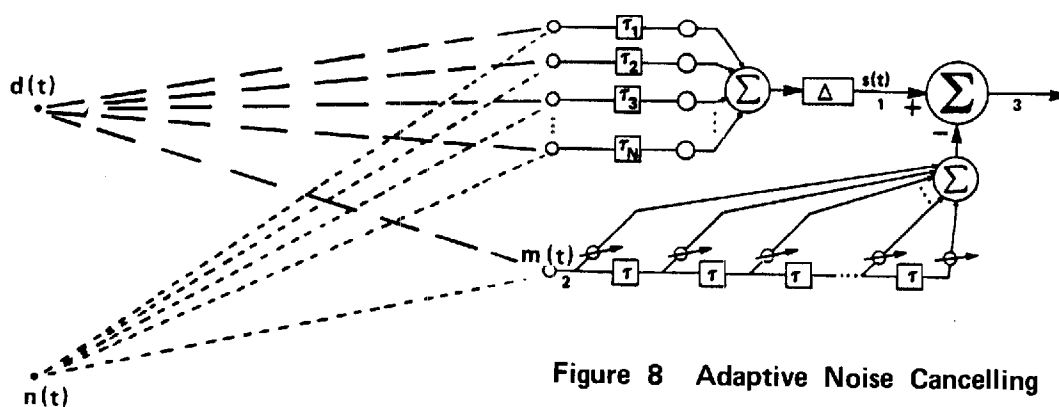


Figure 8 Adaptive Noise Cancelling

Figure 8 shows a block diagram of an adaptive noise canceller together with a constant nonadaptive beamformer whose output is fed to the primary input (point 1). Let  $s(t)$  be the desired signal and  $n(t)$  the undesired one. The reference input,  $m(t)$ , at point 2 goes through a tapped delay line with adjustable weights that are adjusted to minimize the output power at point 3. The higher the correlation between the reference and the primary inputs, the more cancellation occurs. But since one is only

interested in undesired-signal cancellation, the optimal situation would be having the reference signal highly correlated with the undesired-signal component in the primary input but uncorrelated with the desired-signal component. Since this is usually not the case, in most cases some signal cancellation will occur.

Figure 9 depicts a model of a measurement situation, where  $K_{11}(z)$ ,  $K_{12}(z)$ ,  $K_{21}(z)$ ,  $K_{22}(z)$  are transfer functions relating the desired and undesired signal components to the two inputs of the system.  $K_{11}(z)$  represents the adding in phase of the desired-signal and  $K_{21}(z)$  represents the adding out of phase of the undesired-signal.

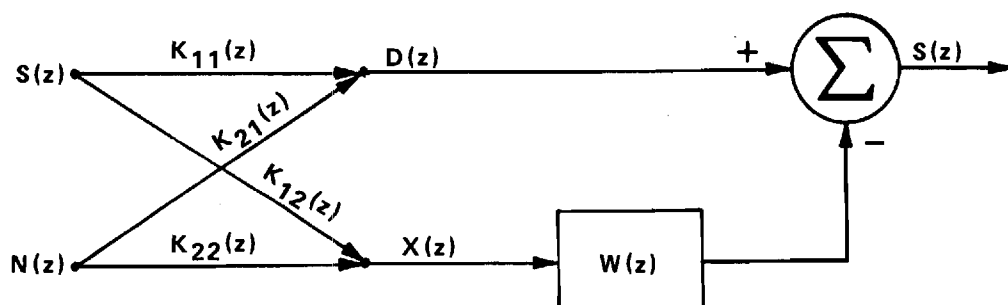


Figure 9 Model of the Transfer Function of the Desired and Undesired Signals,  $s(n)$  and  $n(n)$ , through the Adaptive Noise Cancelling

We have

$$D(z) = S(z) K_{11}(z) + N(z) K_{21}(z) \quad (28)$$

$$X(z) = S(z) K_{12}(z) + N(z) K_{22}(z) \quad (29)$$

If  $S_{gg}$  is the power spectrum of  $g(n)$ , we have

$$\begin{aligned} S_{xx}(z) &= S_{ss}(z) K_{12}(z) K_{12}(1/z) + S_{nn}(z) K_{22}(z) K_{22}(1/z) \\ &\quad + S_{sn}(z) [K_{12}(z) K_{22}(1/z) + K_{12}(1/z) K_{22}(z)] \end{aligned} \quad (30)$$

$$\begin{aligned} S_{dd}(z) &= S_{ss}(z) K_{11}(z) K_{11}(1/z) + S_{nn}(z) K_{21}(z) K_{21}(1/z) \\ &\quad + S_{sn}(z) [K_{11}(z) K_{21}(1/z) + K_{11}(1/z) K_{21}(z)] \end{aligned} \quad (31)$$

$$\begin{aligned} S_{xd}(z) &= S_{ss}(z) K_{11}(z) K_{12}(1/z) + S_{nn}(z) K_{21}(z) K_{22}(1/z) \\ &\quad + S_{sn}(z) [K_{21}(z) K_{12}(1/z) + K_{11}(z) K_{22}(1/z)] \end{aligned} \quad (32)$$

$W(z)$  is an adaptive filter that converges to the Wiener filter,

$$W_{\text{opt}}(z) = \frac{S_{xd}(z)}{S_{xx}(z)} \quad (33)$$

What is of major concern here, is the desired-signal to undesired-noise ratio at the output and also the proportion of desired-signal cancellation that occurs in the

processing. We will look at the case when the reference input is taken from one of the inputs to the beamformer of Figure 8. In that case  $K_{12}(z) = K_{22}(z)$ . We now have from Figure 9,

$$\text{SNR}_{\text{out}}(z) = \frac{S_{ss_{\text{out}}}(z)}{S_{nn_{\text{out}}}(z)} = \frac{S_{ss}(z) |K_{11}(z) - K_{12}(z) W(z)|^2}{S_{nn}(z) |K_{21}(z) - K_{22}(z) W(z)|^2} \quad (34)$$

By using  $W(z) = W_{\text{opt}}(z)$  and  $K_{12}(z) = K_{22}(z)$ , one gets after some calculations,

$$\text{SNR}_{\text{out}}(z) = \frac{1}{\text{SNR}_{\text{ref}}} \quad (35)$$

where  $\text{SNR}_{\text{ref}}$  is the desired-signal to undesired-noise ratio at the reference input.

Now we will look at the proportion of desired-signal cancellation that may occur. Let  $\text{DCANC}(z)$  represent the ratio of the desired-signal component that comes out of the adaptive filter, and the desired-signal component at the primary input.

$$\text{DCANC}(z) = \frac{S_{ss}(z) |K_{12}(z) W(z)|^2}{S_{ss}(z) |K_{11}(z)|^2} \quad (36)$$

Again using  $K_{12}(z) = K_{22}(z)$  and  $W(z) = W_{\text{opt}}(z)$  we get

$$\text{DCANC}(z) = \left| \frac{\frac{S_{ss}(z)}{S_{nn}(z)} \frac{K_{21}(z)}{K_{11}(z)} \frac{S_{sn}(z)}{S_{nn}(z)} \left[ \frac{K_{21}(z)}{K_{11}(z)} + 1 \right]}{\frac{S_{ss}(z)}{S_{nn}(z)} + 1 + 2 \frac{S_{sn}(z)}{S_{nn}(z)}}} \right|^2 \quad (36)$$

The ratio  $K_{21}(z) K_{11}(z)$  represents the improvement of the desired-signal to undesired-noise ratio at the primary input due to the beamforming. The better the beamformer performs the less desired-signal cancellation occurs.

Thus in order to get good results from the adaptive noise canceller, the following is desirable:

- 1). Low desired-signal to undesired-noise ratio, SNR, at the reference input.
- 2). High Desired-signal to undesired-noise ratio at the primary input, i.e. low  $K_{21}(z)/K_{11}(z)$ .
- 3). Low correlation between the desired-signal and the undesired-noise.

## CHAPTER IV

## ACOUSTIC NOISE MEASUREMENTS

There exist International Standards (ISO) that determine procedures that must be followed in measuring sound power levels of noise sources. Any "in situ" method must yield results which are comparable to standard measurements. In these standards the computation of sound power from sound pressure measurements is based on the premise that the mean square sound pressure averaged in time and space,  $\langle \bar{p}^2 \rangle$  is

- 1). Directly proportional to the sound power output of the source.
- 2). Inversely proportional to the equivalent absorption area of the room.
- 3). Otherwise depends only on the physical constants of air density and velocity of sound.

According to these international standards, the analysis is to be done in frequency bands, whose width is either octave or one third octave. Let  $p(t)$  be the sound pressure as a function of time. By dividing  $p(t)$  into its frequency components or certain contiguous frequency bands, one gets

$$p(t) = \sum p_i(t) = \sum p_b(t) \quad (38)$$

where  $N$  is the number of frequency components in  $p(t)$  and  $B$  is the number of contiguous frequency bands, yet to be specified. Since these frequency bands are disjoint, then by squaring and averaging over time, one gets

$$(p(t)^2)_{av} = \sum (p_i(t)^2)_{av} = \sum (p_b(t)^2)_{av} \quad (39)$$

As mentioned earlier the standard bands are either octave or one third octave bands.

If  $f_L(b)$  is the lower frequency boundary of band  $b$ , and  $f_H(b)$  is the upper frequency boundary, then the center frequency of band  $b$  is defined as the geometric mean of  $f_L(b)$  and  $f_H(b)$ , that is

$$f_c(b) = [f_L(b) f_H(b)]^{1/2} \quad (40)$$

Since any two frequencies  $f_1$  and  $f_2$  that satisfy  $f_2 = 2 \cdot f_1$  are said to be one octave apart, an octave band is any band that satisfies  $f_H = 2 \cdot f_L$ . Similarly  $1/N$ 'th octave band is defined



Band no.	Frequency, Hz		
	Center	Lower	Upper
12	16†	14.0	18.0
13	20	18.0	22.4†
14	25	22.4†	28.0
15	31.5†	28.0	35.5
16	40	35.5	45†
17	50	45†	56
18	63†	56	71
19	80	71	90†
20	100	90†	112
21	125†	112	140
22	160	140	180†
23	200	180†	224
24	250†	224	280
25	315	280	355†
26	400	355†	450
27	500†	450	560
28	630	560	710†
29	800	710†	900
30	1,000†	900	1,120
31	1,250	1,120	1,400†
32	1,600	1,400†	1,800
33	2,000†	1,800	2,240
34	2,500	2,240	2,800†
35	3,150	2,800†	3,550
36	4,000†	3,550	4,500
37	5,000	4,500	5,600†
38	6,300	5,600†	7,100
39	8,000†	7,100	9,000
40	10,000	9,000	11,200†
41	12,500	11,200†	14,000
42	16,000†	14,000	18,000
43	20,000	18,000	22,400†
44	25,000	22,400†	28,000
45	31,500†	28,000	35,500

† Also an appropriate quantity for an octave band. The 1000-Hz octave band, for example, has lower and upper frequencies of 710 and 1400 Hz.

Table 1 Standard Center, Lower, and Upper  
Frequencies for Octave and 1/3 Octave Bands [11]

as  $f_H = 2^{1/N} f_L$ .

Table I shows standard center frequencies and the corresponding upper and lower frequencies for one third octave and octave bands. These standard center frequencies are based upon the formula

$$f_c(b) = 10^{b/10} \quad (41)$$

for any band  $b$ .

Most standards for acoustic noise are expressed in terms of sound pressure level, which is defined as

$$L_p = 10 \log \frac{(p(t)^2)_{av}}{p_{ref}^2} \quad (42)$$

and has the units of decibels (dB). The reference pressure  $P_{ref}$  is generally taken to be  $2 \cdot 10^{-5}$  Pascals and corresponds to  $L_p = 0$ .

The range of audible frequencies for people with acute hearing is shown in Figure 10. This figure shows the threshold of hearing as a function of frequency. The ear is most sensitive to frequencies around 3000 Hz but 10000 and 100 Hz are the upper and lower boundaries. Because of the nonuniformity of the sensitivity threshold, the measured sound pressure level is not particularly meaningful unless

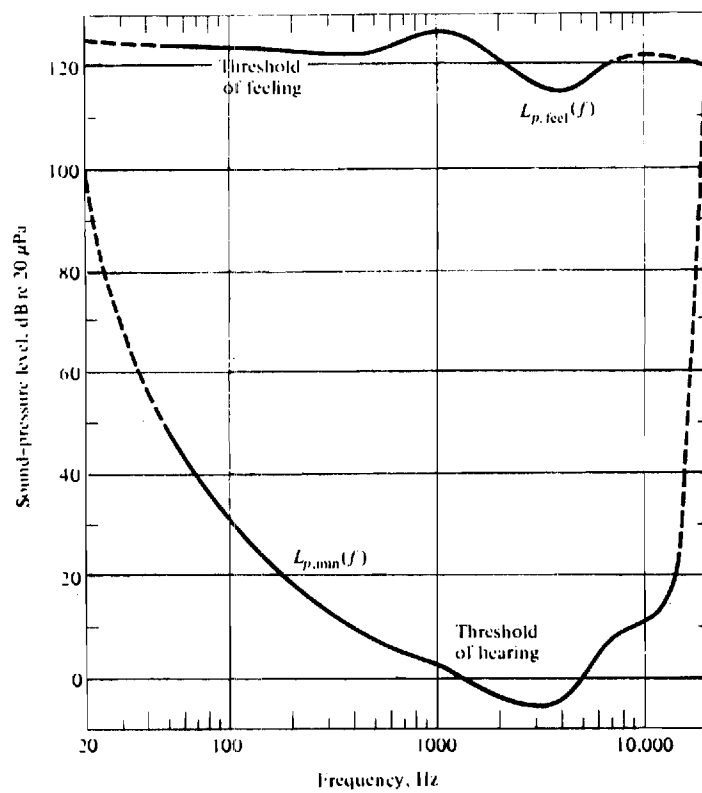


**Figure 10 Frequency-Dependent Thresholds of Hearing and Feeling for People with Acute Hearing [11]**

the frequency or frequency range, at which it was measured, is specified. To compensate for this nonuniformity, a weighted sound pressure level is commonly used, denoted by  $(p(t)^2)_{av,w}$  where

$$(p(t)^2)_{av,w} = \sum w(f_n) (p_n(t)^2)_{av} \quad (43)$$

or

$$L_{p,w} = L_p + \Delta L_w(f) \quad (44)$$

Figure 11 shows three common weighting functions, A, B, and C weighting. Of these three, the A-weighting is the most often used, and is approximately equal to the sensitivity function of the ear, i.e. the negative of Figure 10. By using this weighting function, sounds at different frequencies which are perceived to be equally loud will have approximately the same weighted sound pressure level,  $L_{p,w}$ .

When measuring noise according to the international standards, certain criteria must be followed. For example the microphone array shall not lie in any plane within  $10^\circ$  of a room surface. No microphone in the array shall be closer than  $\lambda/2$  to any room surface of the reverberant room,

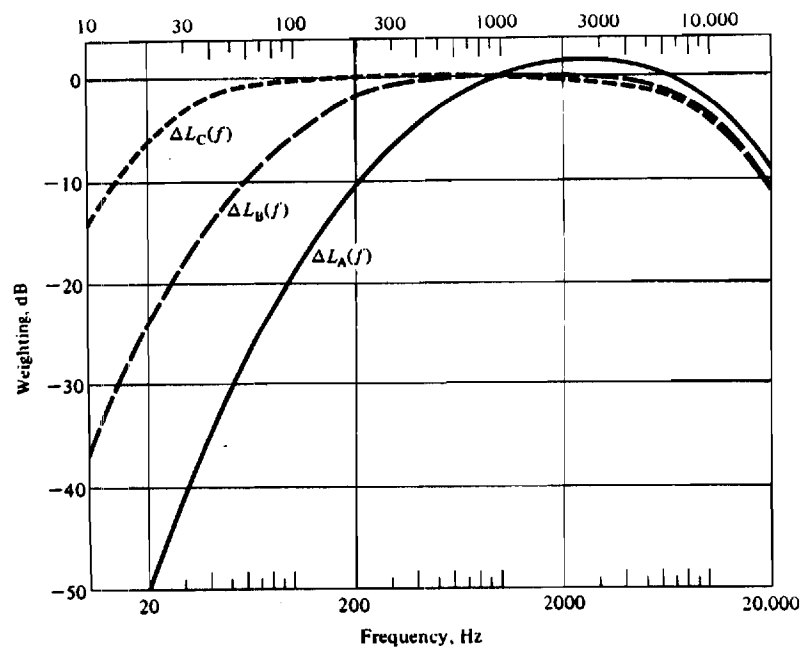


Figure 11 Relative Response Functions  
for A, B, and C Weightings [11]

where  $\lambda/2$  is the wavelength of sound corresponding to the center frequency of the lowest frequency band of interest. The location of the microphone array shall be within that portion of the test room where the reverberant sound field dominates. An array of at least three fixed microphones or microphone positions spaced at least a distance of  $\lambda/2$  from each other, where  $\lambda$  is the wavelength of the sound wave corresponding to the lowest frequency of the frequency band of interest, may be used. Other measurement conditions are specified in the International Standards [5-9].

## CHAPTER V

## ROOM ACOUSTICS

The sound at a point in a room consists of the sound coming directly from the source together with the reflections from walls and objects that may be in the room. These reflections or echoes together with the original sound comprise reverberant sound and the corresponding room is called a reverberant room. It is possible to design a room in such a way that little reverberation occurs. Such a room is called an anechoic room but these rooms are very expensive. All normal rooms are reverberant, but the amount of reverberation depends upon the size of the room, the material that covers the walls (the reflection constants of the walls) and also on any objects that may be in the room. The amount of reverberation is described by the reverberation time of the room. The reverberation time is defined as the time it takes the average sound pressure to drop by 60 dB, which can be directly measured (Figure 12). Figure 12 shows how the reverberation time,  $T_{60}$  is determined. This is not a simple measurement and several attempts have been made in order to try to predict the reverberation time of a specific room from its reflection constants, volume and surface area.

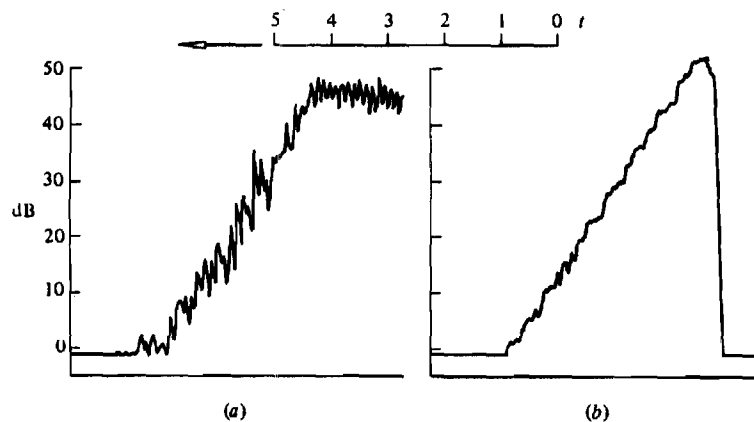


Figure 12 Reverberant Decay of Running Time Average of Square of Acoustic Pressure as Displayed by a High-Speed Level Recorder. (a) Sudden Turnoff of a Narrow-Band Source ( $1000 \pm 50$  Hz) and (b) Firing a Pistol Shot (600 to 1200 Hz) [11]

$$T_{60} = \frac{.161 \text{sec/m}^3 V}{\sum_i \alpha_i A_i} \quad (\text{Sabine}) \quad (45)$$

$$T_{60} = \frac{55.3 V}{c A_s} \quad (\text{Sabine} - \text{Franklin}) \quad (46)$$

$$T_{60} = \frac{13.82 V}{c S [-\ln(1 - \bar{\alpha})]} \quad (\text{Norris} - \text{Eyring}) \quad (47)$$

V: Room volume  $\text{m}^3$

S: Area of room  $\text{m}^2$

$A_i$ : Area of wall  $i$   $\text{m}^2$

$A_s: \sum_i \alpha_i A_i$

$\alpha_i$ : Absorption constant of wall  $i$

$\bar{\alpha}$ : Average absorption constant of walls

c: Speed of sound in air



The first two equations predict a longer reverberation time than the third one does. In that respect, the Norris-Eyring equation overcomes some of the limitations that have been found in the derivation of Sabine's equations, since the Sabine equations have often been found to predict a higher reverberation time than is experimentally measured [11], but for large reflection constants the Sabine equations are more accurate.

The acoustic power  $P$  of the source will spread out in all directions, and at a certain distance from the source,  $r$ , the time averaged radial component of the intensity will be

$$\frac{P_{av} Q_{\theta}}{4 \pi r^2} \quad (48)$$

where  $Q_{\theta}$  is the directivity factor of the source. It is a function of direction and its integral over all solid angles pointing from the source into the room is  $4 \pi$ . For a spherically symmetric source signal  $Q_{\theta} = 1$ . The closer one is to the source, the stronger the intensity of the direct field. If the local spatial average,  $\bar{P}^2$ , of the mean squared pressure is defined as the sum of the direct-field and the reverberant field contributions, then we have

$$\bar{p}^2 = \rho_c P_{av} \left( \frac{Q_\theta}{4 \pi r^2} + \frac{4}{R_{rc}} \right) \quad (49)$$

where  $R_{rc}$  called the room constant is defined as:

$$R_{rc} = \frac{\bar{\alpha} S}{1 - \bar{\alpha}} \quad (50)$$

The radius of reverberation or critical radius is defined as the distance from the source where the direct field and the reverberant field are of equal contribution, i.e.

$$\frac{Q_\theta}{4 \pi r^2} = \frac{4}{R_{rc}}$$

or

$$r_c = \left( \frac{R_{rc} Q_\theta}{16 \pi} \right) \quad (50)$$

For  $r < r_c$  the direct field dominates and for  $r > r_c$  the reverberation field dominates. Figure 13 compares the direct plus reverberant field with the direct field only, inside and outside the radius of reverberation. At  $r = r_c$

the two fields are equally strong and the sound pressure level is 3dB higher than contributed from each one alone.

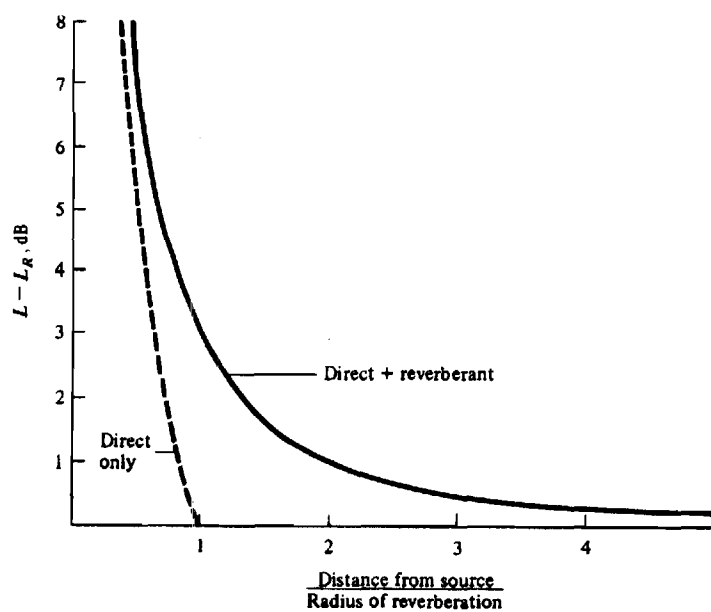


Figure 13 Sound-Pressure Level (Relative to that of Reverberant Field) versus Ratio of Distance  $r$  from Source, to Radius of Reverberation  $r_c$   
Function Plotted is  $10 \log[(r_c/r)^2]$  [11]

## CHAPTER VI

### SIMULATIONS

In this study no real acoustic measurements were carried out due to the complexity of the measurement apparatus required for multi-channel recording of acoustic signals. Instead all the measurements were simulated on the Digital Signal Processing Laboratory Computer Facility. What made these simulations possible was already existing algorithm by J.B.Allen [1] for simulating room effects.

This room simulation algorithm calculates the path of an impulse from one specified source location to a specified observer location. The length of this impulse response is specified so the reverberation time is limited by the length of the impulse response of the room. This algorithm does not take into account any reflecting surfaces except for the walls, ceiling and the floor of the specified room. In a real room there would usually be some other reflecting surfaces, which in that case would shorten the reverberation time of the room. The source is assumed to be a point source and the observer (microphone) is assumed to be omnidirectional. In real measurements, the microphones would usually be directional and the source might not be a point source.

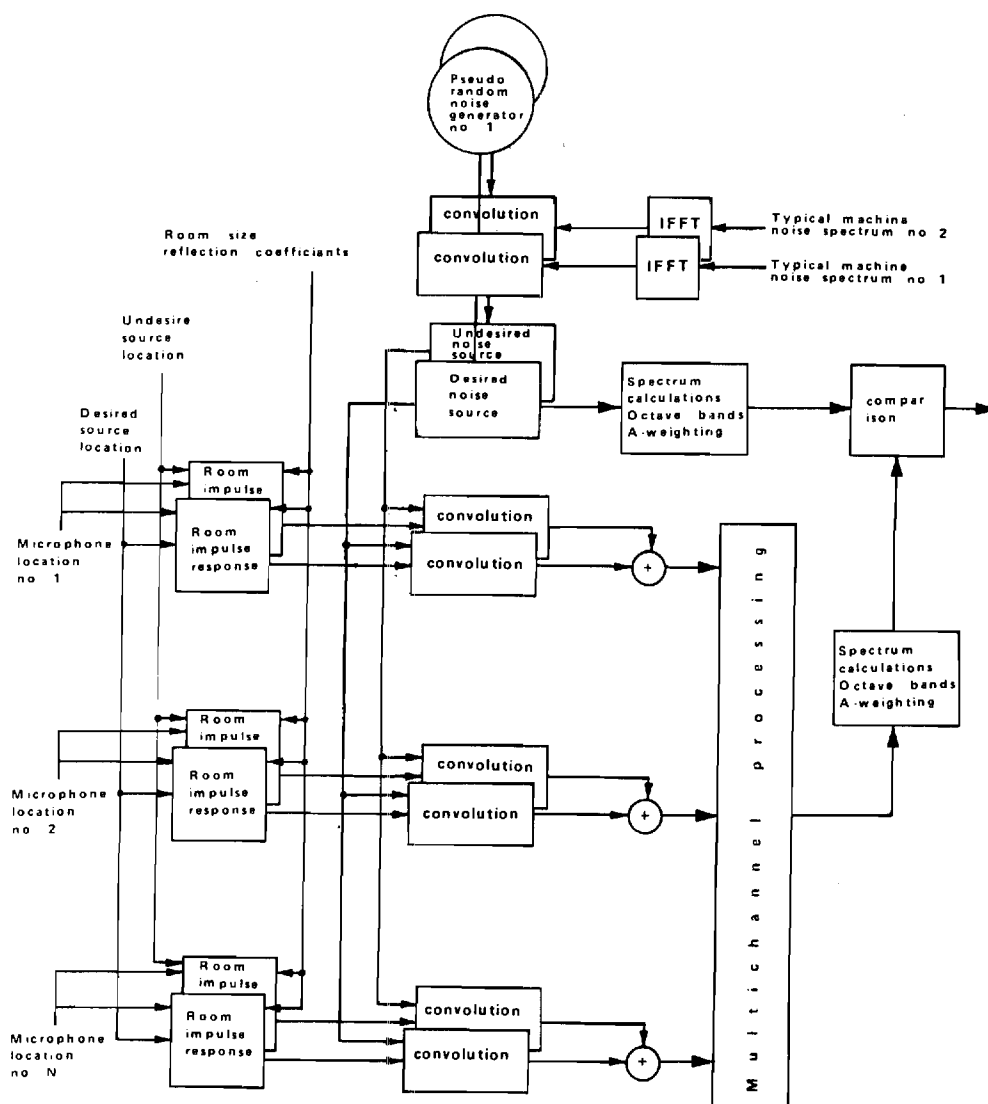


Figure 14 Model of the Procedure for the Simulated Measurements

All these things make our simulated measurements different from real measurements, but the simulations should still give a rather good idea of how well the different processors can achieve the desired goal.

Figure 14 shows a block diagram of all the simulations. First of all the source signals are simulated by convolving pseudo-random white noise with the impulse response of a filter which shapes the frequency spectrum to simulate a typical machine noise spectrum. In cases of more than one source in the room, the same procedure is used to produce all the source signals, but different machine noise signals are used and the pseudo-random noise sources are uncorrelated. This first step gives the desired signal and if needed other signals (undesired ones) that are uncorrelated with each other.

Step number two is to produce the room impulse response for the given characteristics of the room where the length of the impulse response, the signal source location, and the microphone location are specified. For each source in the room, the impulse response of the room must be calculated corresponding to each microphone location. Figure 15 shows one of the simulated room impulse responses.

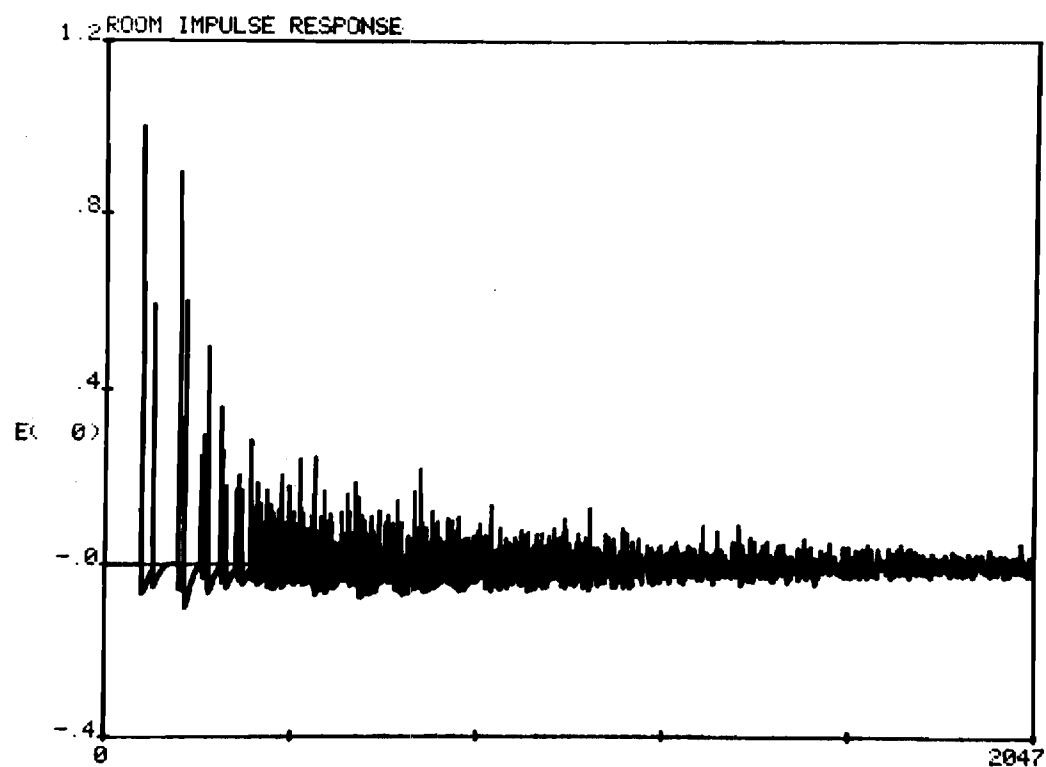


Figure 15 Example of a Simulated Room Impulse Response (Table 3)

Finally, after having produced all these room impulse responses, each of them is convolved with the signal corresponding to the source location. If there is more than one source in the room, all the signals that were simulated for each of the microphones are summed and fed into the corresponding input of the multichannel processor. This procedure simulates a signal at each of the microphone locations, which consists of direct paths from all the sources in the room plus the reverberation paths.



## CHAPTER VII

### EXPERIMENTS

#### Measurement Parameters

All the experiments were conducted on the Digital Signal Processing Laboratory using simulated measurements at an array of microphones. In performing these experiments, there were several parameters to vary, such as the size of the room, the reflection coefficients of the walls of the room, the length of the room impulse response, the location of each source in the room and also the location of the microphone array. In designing the set up, an attempt was made to follow as closely as possible the set up specified in the International Standards for determination of sound power levels of noise sources as described in Chapter IV.

As mentioned in Chapter IV, the algorithm of Allen only describes the path between a source and an observer; i.e. as if there was nothing else in the room to reflect the signals except the walls of the room. In "in situ" measurements, there would usually be other objects, such as noise sources or passive objects like chairs or tables, that would decrease the reverberation time. Apart from these practical considerations there are also some technical

obstacles for doing research on signals that correspond to long reverberation times. The assumption for convergence of the adaptive processors is that the adjacent samples of the different signals in the updating procedure are uncorrelated. This means that when we have long reverberation signals, the time between updatings would have to be long, and therefore convergence would be very slow. Figure 16 shows how the output power converges to its minimum when plotted as a function of number of adaptation, in one of the experiments.

Based on these facts, most of the experiments were conducted with the impulse response of the room shorter than what the equations of reverberation time in chapter V predicted for an empty room with one source and one observer.

The spacing between the microphones is of major concern here since one is dealing with broad band signals. As mentioned in chapter IV the spacing should be  $\frac{\lambda}{2}$  where  $\lambda$  is the lowest wavelength in the frequency band of interest. There are two ways of conducting the measurements. One way is to choose a single spacing for the entire frequency range of interest. A better, but much more complicated method is to use a different spacing for each octave band. In our experiments we used only one set of

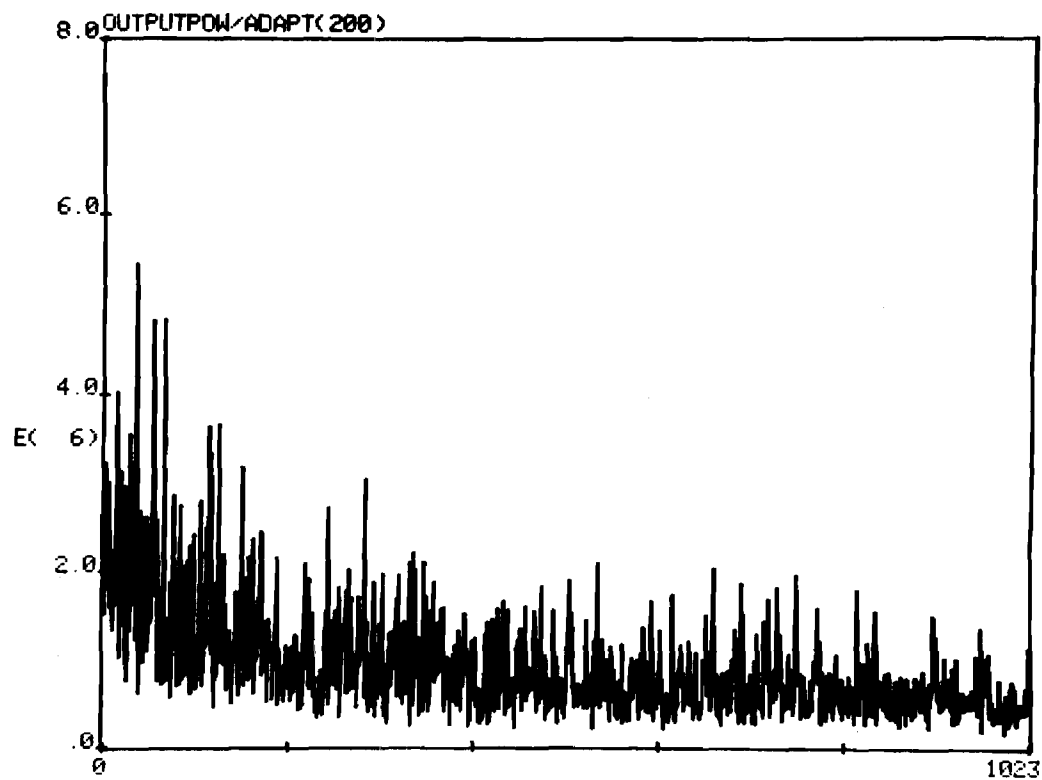


Figure 16 Convergence of the Output Power for one of the Cases  
(Table 5,  $T_a=256$ ,  $\text{Del}=200$ )

spacing (the optimum for band 1) when experimenting with different parameters, but when testing how well each of the techniques could perform, the spacing was optimized for each band.

The number of microphones one can have is limited by the size of the room and the frequency range of interest, since the spacing between them must be at least  $\lambda/2$ , where  $\lambda$  is the wavelength of the lowest frequency of interest. It is also limited by the fact that no microphone can be closer to any wall of the room than  $\lambda/2$  where  $\lambda$  is the wavelength of the center frequency of the lowest band of interest. All the microphones were placed at a distance from the desired source that was larger than the critical radius, so they were in the field of dominating reverberation compared to the desired source.

#### Processor Parameters

For the adaptive processors, the time between adaptations must be long enough so that all successive samples are uncorrelated. Thus the adaptation time depends upon the input signal, the reverberation time and the length of the tapped delay line. For both the adaptive processors, the tapped delay line was chosen long enough to include the reverberation time of the room. For the constrained adaptive beamformer, we chose the constraints that the first row sums up to 1, and the other rows sum up to 0. The

signal from the desired direction propagates then through the filter with unity gain, that is, with no spectral filtering. The time delay of each tap in the tapped delay lines was chosen to be one sample, in order to accomplish maximum resolution in the filtering.

The performance of each processor was tested by varying the parameters in order to get a better feeling of their limitations. The results of the experiments are given in forms of tables, where in each table all parameters are specified, both processor parameters and measurement parameters.

## Experimental Results

### Introduction

All the results are shown in table forms of A-weighted octave band power levels. Since both the A-weighting and the wider measurement bands emphasize the higher frequency bands, the real signal may have low amplitude in the higher bands, but yet appear in the tables just as strong in the higher frequency bands as it is in the lower frequency bands. If we look at the desired and undesired octave band levels, and undo the A-weighting and the frequency summation in each band where the frequency range of the bands increases with higher frequency bands, we will see that both the desired and undesired signal sources have their power

concentrated in the lower frequency bands. The difference between the desired and the undesired signal sources is much bigger in the lower bands than it is in the higher bands, and therefore the improvement that the adaptive processors can accomplish from what the nonadaptive beamformer could, is much larger in the lower frequency bands, than it is in the higher ones.

#### Desired Source + Reverberation

In this case there are no undesired noise sources in the room, the only undesired noise is the reverberation due to the desired noise source. The undesired signal is therefore only a sum of delayed versions of the desired signal. In cases like this where there is no dominating undesired direction i.e., the reverberation echoes are coming from all directions, the equally weighted nonadaptive beamformer gives the best results. Table 2 shows a comparison of the adaptive beamforming and the equally weighted nonadaptive beamforming, where we have a long room impulse response (2048 samples, at a sampling rate of 2000 Hz). From Table 2 one can see that there is no significant improvement using the adaptive beamforming in this case. The adaptive noise canceller is not applicable for this case, since the desired-signal-to-undesired-noise ratio is not low enough, it would have to be less than one to get any improvement at all. From Table 2 one can see that the

equally weighted nonadaptive beamformer performs very well for this situation. This experiment was done using the optimum microphone spacing for the lowest band. In the lowest band the measured signal is 76.94 dB where the processed signal is 74.94 dB and the desired signal is 74.49 dB, so the difference is only .5 dB. The equally weighted nonadaptive beamformer was also tested in worse conditions, i.e. with reflection coefficients .9 and .8, and with room impulse response of 2048 samples. Table 3 shows the results of that experiment. In this case the microphone spacing was optimized for each band. Due to these high reflection coefficients, the measured signal is up to 9 dB higher than the desired signal. From the Table, one can see that after the processing the difference is down to less than 3 dB.

These results show that using only equally weighted nonadaptive beamforming, significant improvements can be accomplished, using only five microphone. The size of the room did not allow more than five microphones in the array in order to be able to process the lowest frequency bands.

#### Desired Source + Reverberation + Undesired Source

In this case, we studied the effect of reverberation as well as an extra undesired noise source. The undesired signal now consists of the reverberation of both of the signal sources in the room and also the direct path of the undesired signal source. Table 4 shows the results of some

tests for the case where the room impulse response has length 2048 samples. The spacing between the microphones was not optimized for each band, but was fixed at the optimum for band 1. In this Table the performance of the adaptive beamformer is shown with different lengths of time between the adaptations. We see that for 256 and 512 samples between adaptations, we get essentially the same results. What this indicates is that the time between adaptations may not be as critical as was expected and that it may not be necessary that the reverberation time is included in the time between adaptation, which would make the adaptive processors much more competitive.

Table 5 shows the results of another experiment where the location of the desired source and the undesired one is different and also the microphone array has a different position. The main difference, however, is that the impulse response of the room is only 256 samples long, so that the reverberation time is somewhat less than that, depending upon the position of the source and the observer. By this, we get a better control over the variables in testing different parameters, since the time between adaptations can now exceed the reverberation time without any difficulties. Again the space between the microphones was the same for all the bands. The value chosen was the optimum for Band one. From Table 5 one can see that the tapped delay line of 400 elements does not improve the results from what they are



using 200 elements in the tapped delay line. The 200 elements delay line includes the reverberation time of most of the sources. By increasing the number of elements to 400 we wanted to test if the adaptive beamformer might be able to improve a broader frequency range than it was capable of, using a 200 element delay line without changing the spacing between the microphones. However, the results did not improve when increasing the taps in the delay line. Having 512 samples between adaptations does not improve the results from the case of 256 samples between adaptations. This further strengthens the results in Table 4 that the time between adaptations does not need to include the length of the tapped delay line plus the whole reverberation time. That is, the simulation indicates that it may only be necessary to include the part of the reverberation where the correlation is strongest.

Table 6 shows a comparison between the three processors; equally weighted nonadaptive beamformer, adaptive beamforming and adaptive noise cancelling, for both four and five microphone array, where the spacing is optimized for each band. The constrained adaptive beamformer gives the best overall results, especially in the lower frequency bands where the difference between the desired and measured signal is high. In the higher frequency bands the adaptation processes did not improve the results over the nonadaptive beamformer. This can be

explained by the fact that the dominating undesired signal source has most of its power distributed at the lower frequency bands, and in the higher frequency band it is the reverberation of the room that becomes dominant, and the equally weighted beamformer is the optimum for such cases. In comparing the results of 4 and 5 sensor arrays, we notice that there is a significant improvement from 4 to 5 microphones in the case of the equally weighted constant beamformer. In the case of adaptive beamformer there is some improvement from a 4 to 5 sensor array, but the difference is not as high as in the case of constant beamformer in the lower bands where the adaptation is active, but in higher frequency bands we get similar improvements as we did for the nonadaptive one. The adaptive noise cancelling improves the results from what they were for the nonadaptive beamformer in the lower bands but in the higher bands, where the reverberation is dominating it does not give any improvement but instead decreases the desired-signal-to-undesired-noise ratio.

Table 7 shows the results where the undesired source is not as strong as it was in Table 5 and 6. The room impulse response is 256 samples long but the reflection coefficients are .9 and .8 instead of .7 and .6 in the two previous examples. The room size, microphone location and desired source location are all the same as they were in Table 3 where we had only reverberation. Part of Table 7 shows a

comparison of results in using 400, 300, and 256 samples between adaptations with the optimum spacing for band 1. There is not much difference in the results in using these three different time intervals between adaptation. This is the same result as in Table 5. The rest of the table is from experiments with 300 samples between adaptation. There we again have a comparison between the three processors, where the spacing is optimized for each band. The difference between the processed signal and the desired one is not as large as it was in Table 6, but on the other hand, the undesired signal noise has much more power in Table 6 than it has in Table 7. However, the reverberation is stronger in Table 7 than it is in Table 6. Here we get very similar results as in Table 6; that is, at lower bands, where the undesired signal source coming from a specific undesired direction is dominating, the constrained adaptive beamformer and the adaptive noise cancelling give very similar results, and improve the results from what they were for the nonadaptive equally weighted processor. However, as before, as the frequency bands get higher, the reverberation takes over and the nonadaptive equally weighted beamformer performs best of the three.

### Computer Time Considerations

In comparing the three processing techniques that we tried, it would be unfair not to mention the computer time that the different techniques require. The nonadaptive equally weighted processor is obviously the simplest one, and the processing time is no factor there. However, we have to pay the price of powerful techniques. The constrained adaptive beamformer, that is applicable for all circumstances, is extremely time expensive, since there is a lot of computation involved due to the huge weight matrix that is implied and is involved in all the calculations. The noise cancelling technique, on the other hand, has only one tapped delay line, and requires therefore only about  $1/N$  times the time that the constrained adaptive beamformer requires, where  $N$  is the number of microphones.

Therefore, when applicable, the adaptive noise cancelling is much more practical to use, not to mention the nonadaptive equally weighted beamformer, but, if we want to pay the price, the constrained adaptive beamformer gives the best overall performance, and the desired signal is assured of going through the process with unity gain.

**TABLE 2 - A Comparison between Nonadaptive Equally Weighted Beamformer and Constrained Adaptive Beamformer in a Reverberant Environment**

**Situation:** Desired signal + reverberation  
Room impulse response 2048 samples  
Microphone spacing optimized for band 1  
Reflection coefficients .7 (walls) and .6 (floor + ceiling)

Band no.	Center freq.	Desired signal	Measured signal	Out of non-adaptive beamf.	Out of Adaptive Ta=512	Beamformer Ta=1024
1	63	74.49	76.98	74.94	74.69	74.68
2	125	79.45	83.57	80.56	80.54	80.62
3	250	81.15	85.24	82.31	82.36	82.33
4	500	77.53	81.12	79.14	79.11	79.12
5	1000	71.64	75.75	73.08	73.07	73.08

**Measurement and processor parameters:**

Room size: 100x120x60 feet<sup>3</sup>  
Desired signal source location: (25,25,10) feet  
Microphone array location: (50,50,30)  $\pm$  K l (.235,-.394,.197)  
Number of microphones in array: 5  
Number of taps in delay line: 200  
Time between adaptation; Ta  
Sampling frequency: 2000 Hz

K: spacing between microphones (samples)  
l: microphone index from the center one

**TABLE 3 - Performance of the Nonadaptive Equally Weighted Beamformer in a Reverberant Environment**

**Situation:** Desired signal + reverberation  
Room impulse response 2048 samples  
Microphone spacing optimized for each band  
Reflection coefficients .9 (walls) and .8 (floor + ceiling)

Band no.	Center freq.	Desired signal	Measured signal	Out of non-adaptive beamf.	Difference before proc.	Difference after proc.	Improve-ment ratio
1	63	75.23	81.98	77.40	6.45	2.17	.68
2	125	79.82	89.05	82.25	9.23	2.43	.74
3	250	80.67	89.28	83.02	8.61	2.35	.73
4	500	77.35	85.51	79.59	8.16	2.24	.73
5	1000	71.57	79.71	74.28	8.14	2.71	.67

**Measurement and processor parameters:**

Room size: 100x120x60 feet<sup>3</sup>  
Desired signal source location: (25,25,10) feet  
Microphone array location: (50,50,30)  $\pm$  K I (.236,-.394,.197)  
Number of microphones in array: 5  
Sampling frequency: 2000 Hz

**TABLE 4 - A Comparison Between Nonadaptive Equally Weighted Beamformer and Constrained Adaptive Beamformer in a Noisy Reverberant Environment**

**Situation:** Desired signal source + undesired signal source + reverberation  
Room impulse response 2048 samples  
Microphone spacing optimized for band 1  
Reflection coefficients .7 (walls) and .6 (floor + ceiling)

Band no.	Center freq.	Desired signal	Undesired signal	Measured signal	Out of non-adaptive beamf.	Out of adaptive Beamformer	
						Ta=256	Ta=512
1	63	74.49	93.82	100.03	93.02	87.90	87.95
2	125	79.45	98.52	104.21	95.79	91.84	91.42
3	250	81.15	93.08	98.68	91.79	91.70	91.60
4	500	77.53	92.56	97.52	89.67	89.62	89.62
5	1000	71.64	87.26	92.69	85.69	85.65	85.66

**Measurement and processor parameters:**

Room size: 100x120x60 feet<sup>3</sup>  
Desired signal source location: (25,25,10) feet  
Undesired signal source location: (25,90,10) feet  
Microphone array location: (50,50,30)  $\pm$  K I (.236,-.394,.197)  
Number of microphones in array: 5  
Time between adaptation: Ta  
Number of taps in delay line: 200  
Sampling frequency: 2000Hz

**TABLE 5 - A Test of Performance by varying processor parameters**

**Situation;** Desired signal + undesired signal source + reverberation  
Room impulse response 256 samples  
Microphone spacing optimized for band 1  
Reflection coefficients .7 (walls) and .6 (floor + ceiling)

Band no.	Center freq.	Desired signal	Undesired signal	Measured signal	Out of adaptive beamformer			Out of adaptive noise cancelling
					Ta=256 Del=200	Ta=512 Del=200	Ta=512 Del=400	
1	63	74.49	93.22	95.61	80.60	81.52	83.08	83.86
2	125	79.45	97.88	100.03	85.00	86.00	87.12	90.14
3	250	81.15	93.47	97.87	88.80	89.01	89.05	88.24
4	500	77.53	92.72	95.76	88.34	88.32	88.45	89.84
5	1000	71.64	97.31	90.76	84.04	84.02	84.28	85.79

**Measurement and processor parameters:**

Room size: 80x120x100 feet<sup>3</sup>  
Desired signal source location: (25,90,50)  
Undesired signal source location: (25,25,50)  
Microphone array location: (50,55,50)  $\pm$  K I (.139,.099,.470)  
Number of microphones in array: 5  
Number of taps in delay line: Del  
Time between adaptaton : Ta  
Sampling frequency: 2000 Hz



**TABLE 6 - Comparison between the three Processing Techniques Using 4 and 5 Microphones array in Noisy Reverberant Environment**

**Situation:** Desired signal + undesired signal source + reverberation  
Room impulse response 256 samples  
Microphone spacing optimized for each band  
Reflection coefficients .7 (walls) and .6 (floor + ceiling)

**a) Equally Weighted Nonadaptive Beamformer**

**i) 5 Microphone Array**

Band no.	Center freq.	Desired signal	Measured signal	Signal after processing	Difference before proc.	Difference after proc.	Improve-ment ratio
1	63	75.28	99.87	85.73	24.59	10.75	.56
2	125	79.94	102.17	86.39	22.23	6.45	.71
3	250	81.03	94.52	85.32	13.49	4.29	.68
4	500	77.54	97.17	82.77	19.63	5.23	.73
5	1000	71.69	90.62	77.62	18.93	5.93	.69

**ii) 4 Microphone Array**

Band no.	Center freq.	Desired signal	Measured signal	Signal after processing	Difference before proc.	Difference after proc.	Improve-ment ratio
1	63	75.28	99.87	89.15	24.59	13.87	.44
2	125	79.94	102.17	89.00	22.23	9.06	.59
3	250	81.03	94.52	86.60	13.49	5.57	.59
4	500	77.54	97.17	85.27	19.63	7.73	.61
5	1000	71.69	90.62	79.56	18.93	7.87	.58

TABLE 6 (continued)

b) Constrained Adaptive Beamformer

i) 5 Microphone array

Band no.	Center freq.	Desired signal	Measured signal	Signal after processing	Difference before proc.	Difference after proc.	Improvement ratio
1	63	75.28	99.87	81.53	24.59	6.25	.75
2	125	79.94	102.17	85.08	22.23	5.14	.77
3	250	81.03	94.52	85.56	13.49	4.53	.66
4	500	77.54	97.17	83.15	19.63	5.61	.71
5	1000	71.69	90.62	77.62	18.93	5.93	.69

ii) 4 Microphone array

Band no.	Center freq.	Desired signal	Measured signal	Signal after processing	Difference before proc.	Difference after proc.	Improvement ratio
1	63	75.28	99.87	82.02	24.59	6.74	.73
2	125	79.94	102.17	86.96	22.23	7.02	.68
3	250	81.03	94.52	86.94	13.49	5.91	.56
4	500	77.54	97.17	85.56	19.63	8.02	.59
5	1000	71.69	90.62	79.66	18.93	7.97	.58

TABLE 6 (continued)

## c) Adaptive Noise Cancelling

## i) 5 Microphone array

Band no.	Center freq.	Desired signal	Measured signal	Signal after processing	Difference before proc.	Difference after proc.	Improvement ratio
1	63	75.28	99.87	82.10	24.59	6.82	.72
2	125	79.94	102.17	86.02	22.23	6.08	.73
3	250	81.03	94.52	86.13	13.49	5.10	.62
4	500	77.54	97.17	84.47	19.63	6.93	.65
5	1000	71.69	90.62	80.12	18.93	8.43	.55

## ii) 4 Microphone array

Band no.	Center freq.	Desired signal	Measured signal	Signal after processing	Difference before proc.	Difference after proc.	Improvement ratio
1	63	75.28	99.87	84.83	24.59	9.55	.61
2	125	79.94	102.17	87.38	22.23	7.44	.67
3	250	81.03	94.52	85.99	13.49	4.96	.63
4	500	77.54	97.17	86.21	19.63	8.67	.56
5	1000	71.69	90.62	80.10	18.93	8.41	.55

Measurement and processor parameters:

Room size: 80x120x100 feet<sup>3</sup>  
 Desired signal source location: (25,90,50)  
 Undesired source location: (24,25,50)  
 Microphone array location: (50,55,50)  $\pm$  K I (.139,.099,.470)  
 Number of taps in delay line: 200  
 Time between adaptation: 256 samples  
 Sampling frequency: 2000 Hz

**TABLE 7 - A Test of Performance by Varying Processor Parameters and a Comparison between the three Different Processing Techniques in a Noisy Reverberant Environment**

**Situation:** Desired Signal + undesired signal source + reverberation  
Room impulse response 256 samples  
Reflection coefficients .9 (walls) and .8 (floor + ceiling)

**a) Microphone spacing optimized for band 1**

Band no.	Center freq.	Desired signal	Undesired signal	Measured signal	Out of Ta=256	adaptive beamformer Ta=300	Ta=400
1	63	75.23	83.67	88.92	78.14	77.77	77.88
2	125	79.81	88.33	95.21	84.52	84.46	85.49
3	250	80.67	83.93	90.34	85.11	85.22	85.55
4	500	77.35	83.17	88.10	82.45	82.43	82.45
5	1000	71.57	77.76	83.78	76.86	76.86	76.85

**Measurement and processor parameters:**

Room size: 100x120x60 feet<sup>3</sup>  
Desired signal source location: (25,25,10)  
Undesired signal source location: (25,90,10)  
Microphone array location: (50,50,30)  $\pm$  (.236,-.394,.197)  
Number of microphones in array: 5  
Number of taps in delay line: 200  
Time between adaptation: Ta  
Sampling frequency: 2000 Hz

TABLE 7 (continued)

b) Microphone spacing optimized for each band  
Time between adaptation 300

Band no.	Center freq.	Desired signal	Undesired signal	Measured signal	Signal after processing	Difference before proc.	Difference after proc.	Improvement ratio
Equally weighted nonadaptive beamformer								
1	63	75.23	83.67	88.92	82.35	13.69	7.12	.48
2	125	79.81	88.33	95.21	85.43	15.40	5.62	.64
3	250	80.67	83.93	90.34	84.18	9.67	3.51	.64
4	500	77.35	83.17	88.10	81.69	10.75	4.34	.60
5	1000	71.57	77.76	83.78	76.78	12.21	5.21	.57
Constrained adaptive beamforming								
1	63	75.23	83.67	88.92	77.77	13.69	2.54	.81
2	125	79.81	88.33	95.21	83.89	15.40	4.08	.75
3	250	80.67	83.93	90.34	83.49	9.67	2.82	.71
4	500	77.35	83.17	88.10	81.86	10.75	4.51	.58
5	1000	71.57	77.76	83.78	76.72	12.21	5.15	.58
Adaptive noise cancelling								
1	63	75.23	83.67	88.92	78.70	13.69	3.47	.75
2	125	79.81	88.33	95.21	84.51	15.40	4.70	.69
3	250	80.67	83.93	90.34	81.80	9.67	1.13	.88
4	500	77.35	83.17	88.10	81.95	10.75	4.60	.57
5	1000	71.57	77.76	83.78	76.78	12.21	5.21	.57

## CHAPTER VIII

### CONCLUSIONS AND RECOMMENDATIONS

#### Conclusions

From the experimental results on the simulated measurements, we have come to the following conclusions:

1. In cases where reverberation is the dominating contribution of the undesired signal noise, the nonadaptive equally weighted beamformer performs just as well as the two complicated adaptive processors, and would therefore be the best one (of these three) to use. How close the processed signal is to the desired signal depends upon the amount of reverberation. That is, the higher the contribution of the undesired signal noise in the measured signal, the poorer results.

2. The time between adaptations did not turn out to be as critical as was expected. In fact, it appears that one can have long reverberation time without having to have the time between adaptations include the whole reverberation time. This makes the adaptive processors much more competitive than they would otherwise be.

3. In cases where we have some undesired signal noise that comes from a specific direction dominating over the reverberation signal, the adaptive processors can improve the measured signal by a considerable amount from what the equally weighted nonadaptive beamformer could accomplish. The stronger the contribution of the undesired signal from the specific direction is in the total undesired signal noise, the more improvement is accomplished using adaptive processors rather than the nonadaptive one. The constrained adaptive beamformer ensures the best performance under all circumstances, but is also the most complicated and requires a long processing time. The two other processors, the nonadaptive equally weighted beamformer and the adaptive noise cancelling, can give just as good performance as the constrained adaptive beamformer for the two extreme cases of dominating reverberation and dominating signal from an undesired direction.

4. We have shown that significant improvement can be accomplished in estimating the desired signal by using beamformers. If this improvement is good enough for making accurate noise measurements in an "in situ" environment is still to be determined. By looking at the results we see that the error is down to .5 dB for some cases but goes up to 5 and 6 dB for other cases, depending on how much relative undesired noise there is in the measured signal. Having an error of 5 or 6 dB could obviously not be

considered an accurate measure of the desired signal. In order to get further improvement one would have to increase the number of microphones and (or) change the form of the array. Increasing the number of microphones would only improve the reverberation part of the undesired signal unless there are more undesired signal sources than microphones. However, the number of microphones allowed, is limited by the size of the room and the lowest frequency band of interest.

### Recommendations

For future research it would be interesting to investigate in different positions of the microphones relative to one another. For example to let them form a plane instead of a line and study what kind of a grid would give the best performance. In this aspect one might try rectangular or hexagonal grid, and study the effects of unequal spacing. It would be interesting to see what kind of results one would get this way. This way one can also have a much larger number of microphones.

Another important problem which remains is to make real measurements in a real environment and compare the results to what was obtained using the simulations.



## APPENDIX

An Approach to Solve the Optimization Problem  
in Hilbert Spaces

The problem we want to solve here is

$$\text{Minimize } w^T R_{xx} w$$

$$\text{subject to } C^T w = f$$

If  $f$  was set equal to zero, we would get the homogeneous form of the constraint equation,

$$C^T w = 0$$

The set of  $w$  that satisfies this equation forms a subspace that we can call  $M$ . That is  $M$  is the set of all  $v$ , such that

$$C^T v = 0$$

$M$  is the null space of  $C^T$ .

$$M = N(C^T) = \{v : C^T v = 0\}$$

The reason we want to define this homogeneous form, is that it forms a subspace. We can find the solution of the unconstrained problem, project it onto the homogeneous constraint subspace, and then shift it by some  $g$ , where  $g$  would be the solution of

$$C^T g = f$$

i.e.

$$g = C (C^T C)^{-1} f$$

$w$  is in a  $NL$  dimensional vector space, that we can call  $H$ ,  $M$ , which we have already seen is the nullspace of  $C$ , i.e.

$$M = N (C^T)$$

Define  $M^\perp$  as the orthogonal complement of  $M$ . That is  $M^\perp$  is the collection of all vectors in  $H$  that are orthogonal to each vector in  $M$ . Symbolically,

$$M^\perp = \{ x: (s, x) = 0, \text{ for all } s \in M \}$$

where  $(x, s)$  denotes the inner product of  $s$  and  $x$ . Since  $M$  is the nullspace of  $C^T$ , it can be shown that  $M^\perp$  is the range of  $C$  i.e.

$$M^\perp = R(C)$$

Now we want to find the projection operator that projects all the vectors in the vector space  $H$  onto the subspace  $M$ . This projection,  $P_M$ , must satisfy

$$C^T(P_M v) = 0 \quad \text{for all } v \in H$$

By defining

$$P_M = I - C(C^T C)^{-1} C^T$$

then

$$P_M v = v - C(C^T C)^{-1} C^T v$$

and

$$C^T(P_M v) = C^T v - C^T C(C^T C)^{-1} C^T v = 0$$

so  $P_M$  is indeed a projection onto  $M$ . To be a projection  $P_M$  must be self-adjoint and  $P_M P_M = P_M$ . It can be easily verified that  $P_M$  satisfies these conditions.

Let  $g$  be a vector in  $H$  satisfying

$$C^T g = f$$

i.e.

$$g = C(C^T C)^{-1} f$$

Now define  $u=w-g$ . That is, if we shift the constraint plane to the homogeneous plane, and the constraints become

$$C^T u = 0$$

that is,  $u$  lies in  $M$  and therefore  $P_M u = u$ . Now we have

$$\begin{aligned} w^T R_{xx} w &= (u + g)^T R_{xx} (u + g) \\ &= u^T R_{xx} u + g^T R_{xx} g + u^T R_{xx} g + g^T R_{xx} u \end{aligned}$$

and since  $R_{xx}$  is symmetric

$$= u^T R_{xx} u + g^T R_{xx} g + 2 u^T R_{xx} g$$

We want to minimize

$$\begin{aligned} &w^T R_{xx} w \\ &= \underset{u}{\text{minimize}} \quad u^T R_{xx} u + 2 u^T R_{xx} g + g^T R_{xx} g \end{aligned}$$

By imposing in the constraints  $P_M u = u$  in the equation, we can solve the unconstrained problem, that is

$$\underset{u}{\text{Minimize}} \quad (P_M u)^T R_{xx} (P_M u) + 2 (P_M u)^T R_{xx} g + g^T R_{xx} g$$

and then use

$$w_{\text{opt}} = P_M u_{\text{opt}} + g$$

Using the gradient method we get

$$\nabla_u [u^T P_M R_{xx} P_M u + 2 u^T P_M R_{xx} g + g^T R_{xx} g] = 0$$

Hence

$$P_M R_{xx} P_M u_{\text{opt}} + P_M R_{xx} g = 0$$

or

$$P_M R_{xx} \underbrace{(P_M u_{\text{opt}} + g)}_{w_{\text{opt}}} = 0$$

that is

$$P_M R_{xx} w_{\text{opt}} = 0$$

which implies that

$$R_{xx} w_{\text{opt}} \in M^\perp = R(C)$$

Therefore we can write

$$R_{xx} w_{\text{opt}} = C h \text{ for some vector } h$$

from which it follows that

$$w_{\text{opt}} = R_{xx}^{-1} C h$$

By multiplying both sides of the above equation by  $C^T$ , we get

$$C^T w_{\text{opt}} = C^T R_{xx}^{-1} C h$$

which implies

$$h = (C^T R_{xx}^{-1} C)^{-1} f$$

Hence

$$w_{\text{opt}} = R_{xx}^{-1} C (C^T R_{xx}^{-1} C)^{-1} f$$

Using the gradient algorithm, we can update the weighting coefficients using

$$w(k+1) = w(k) - \mu \nabla_w [ w^T(k) R_{xx}(k) w(k) ]$$

where  $\mu$  is the step size. To confine the updated weights to the constrained plane, they are projected onto the constraint subspace,  $C^T w = 0$  and then shifted it by  $g$ . That is

$$w(k+1) = P_M [ w(k) - \mu x(k)y(k) ] + g$$

Now using the approximation that

$$R_{xx}(k) = x(k) x^T(k)$$

and also using

$$y(k) = x^T(k) w(k)$$

we get

$$w(k+1) = P_M [ w(k) - \mu x(k)y(k) ] + g$$

As initial conditions one can use

$$w(0) = g$$

since this choice satisfies the constraints. The overall adaptive algorithm is then

$$w(0) = g$$

$$w(k+1) = P_M [ w(k) - \mu x(k)y(k) ] + g$$

## BIBLIOGRAPHY

- [1] J.B.Allen and D.A.Berkely, "Image Method for Efficiently Simulating Small-Room Acoustics", J.A. Acoust. Soc. Am., 5(4), April 1979.
- [2] O. L. Frost, III, "An Algorithm for Linearly Constrained Adaptive Array Processing", Proc. IEEE, Vol. 60 pp. 926-935, August 1972.
- [3] B.Widrow, et al., Adaptive Noise Cancelling: Principles and Applications", Proc. IEEE, Vol. 63, pp.1692-1716, December 1975.
- [4] ANSI SI.29-1979, Noise Emitted by Computer and Business Equipment, American National Standards Institute, New York, New York 10018.
- [5] ISO 3741-1975, Acoustics-Determinating of Sound Power Level of Noise Sources-Precision Methods for Broad-Band Sources in Reverberation Rooms.
- [6] ISO 3742-1975, Acoustics Determination of Sound Power Level of Noise Sources-Precision Methods for Discrete-Frequency and Narrow-Band Sources in Reverberation Rooms.
- [7] ISO DIS 3744, Acoustics-Determination of Sound Power Levels of Noise Sources-Engineering Methods for Free Field Conditions Over A Reflecting Plane.



- [8] ISO 3745-1977, Acoustics-Determination of Sound Power Levels of Noise Sources-Precision Methods for Anechoic and Semi-Anechoic Rooms.
- [9] ISO DIS 3744 Acoustics-Determination of Sound Power Levels of Noise Sources-Engineering Methods for Free Field Conditions Over a Reflecting Plane.
- [10] R. A. Monzingo and T. W. Miller, Introduction to Adaptive Arrays, John Willey & Sons, Inc. 1980.
- [11] A.D. Pierce, Acoustics, McGraw-Hill Book Company, New York, 1981